# Proton and Ion Linear Accelerators

## Week 2, part 3

**Yuri Batygin and Sergey Kurennoy**
**LANL**

June 25, 2019


National Nuclear Security Administration
Operated by Los Alamos National Security, LLC for the U.S. Department of Energy's NNSA

LA-UR-19-24870

# Proton and Ion Linear Accelerators – Week 2, Part 3

- **Why linacs & RF together?**
- **Reminder: basics of linacs**
- **RF cavities**
- **Accelerating structures: RFQ, DTL, CCL, etc.**
- **Electromagnetic (EM) design of accelerating structures. SF**
- **Linac components**

**Sources:**

T.P. Wangler. *RF linear accelerators*, Wiley-VCH, 2nd Ed., 2008.

*Handbook of Accelerator Physics and Engineering*. Eds. A. Chao *et al*. World Scientific, 2013.

# Figures of merit for accelerating structures

Quality factor (stored energy $U$, averaged power loss $P$)

$$Q = \frac{\omega U}{P}$$

Shunt impedance (total cavity voltage $V_0$)

$$R_{sh} = \frac{V_0^2}{P}$$

Effective shunt impedance (effective voltage $V_0 T$)

$$R_{eff} = R_{sh} T^2$$

Shunt impedance per unit length (voltage $V_0 = E_0 L$)

$$Z = \frac{E_0^2}{P / L}$$

Effective shunt impedance per unit length ($Z_{\text{eff}}$)

$$ZT^2 = \frac{\left(E_0 T\right)^2}{P / L}$$

Ratio $R_{\text{eff}}/Q$ is independent of surface losses and depends only on the cavity (structure) geometry

$$\frac{R_{eff}}{Q} = \frac{\left(V_0 T\right)^2}{\omega U}$$

Ratios $E_{max}/E_{acc}$ ($E_{acc}=E_0 T$) and $B_{max}/E_{acc}$ – lower is better.
The latter is very important for SC cavities.

# Linac parts

Linac scheme: particle source + accelerating structure(s)

Electron linacs: electron gun + linac (TW or SW $\beta$=1 structure); with some tricks.

Ion linacs: ion source (injector) + various structures for different values of $\beta$.

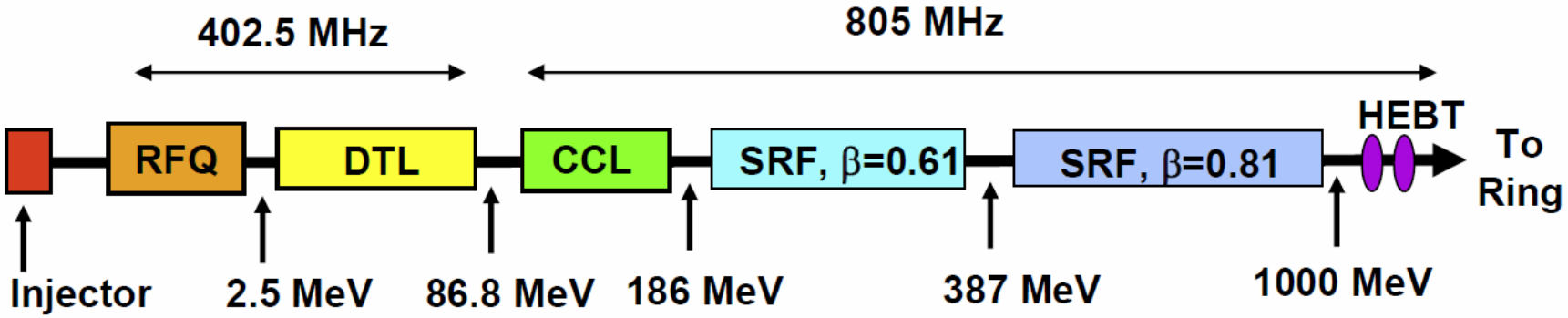


Scheme of SNS linac:

- RFQ = RF Quadrupole accelerator
- DTL = Drift-Tube Linac
- CCL = Coupled-Cavity Linac
- SRF = SC RF linac
- HEBT = High-Energy Beam Transport

# Typical RF linac structures

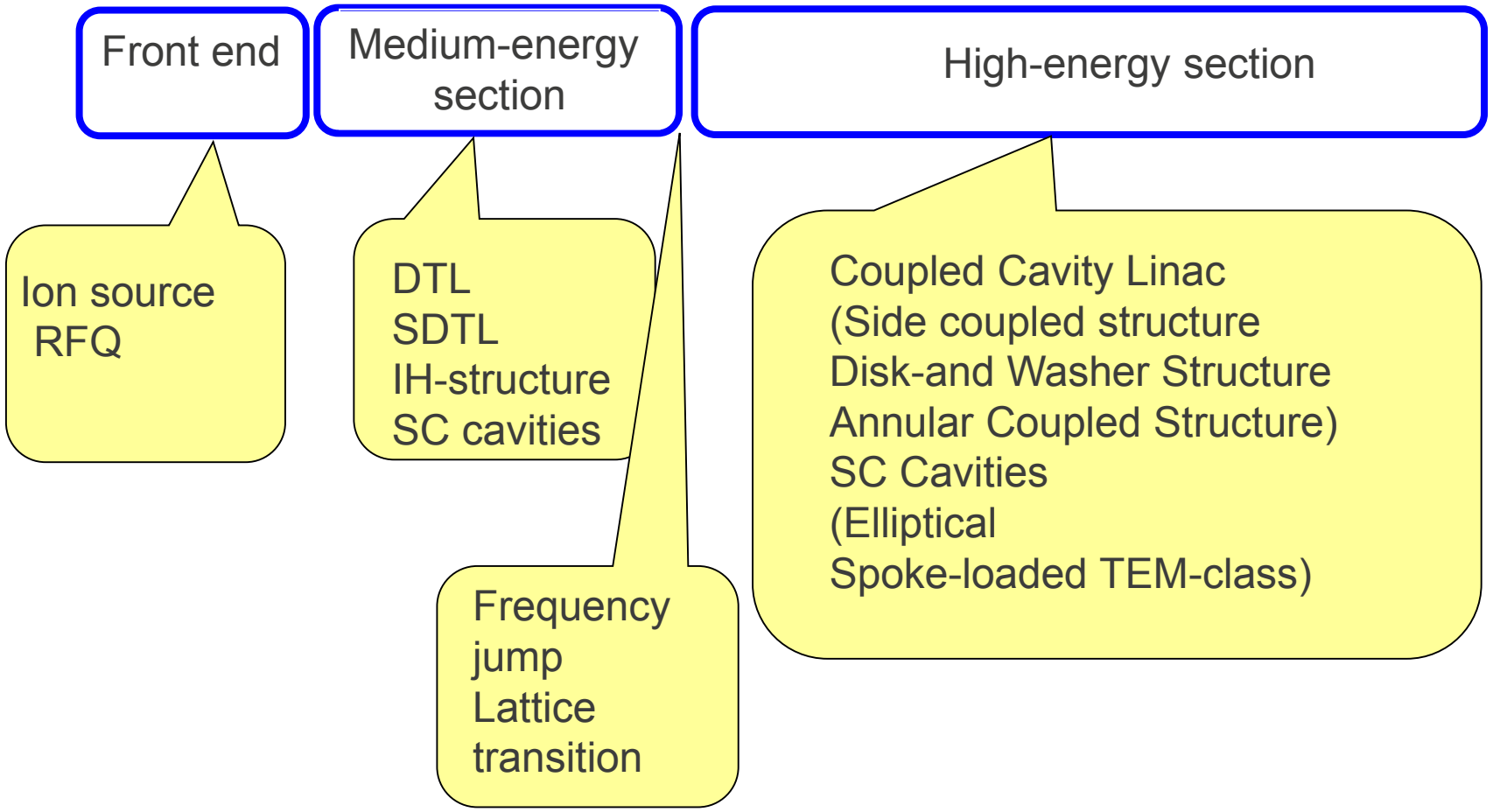


From P. Ostroumov (2012)

# RF Linac Types

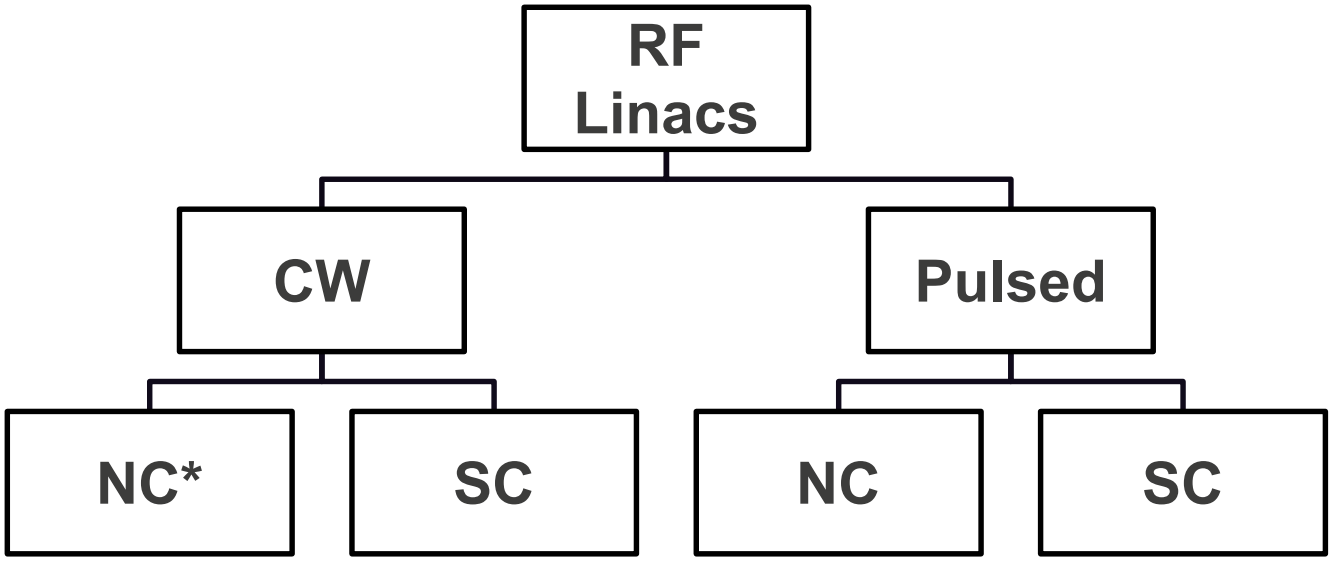


**ISAC-I**
**RIKEN inj.**
**LEDA RFQ**
**SARAF RFQ**

*Low-energy, several MeV/u Heavy-ions

**ATLAS**
**ISAC-II**
**INFN**
**SARAF**
SPIRAL-2
FRIB
Project X
EURISOL
ADS projects

**LANSCE**
**Synchrotron Injectors (FNAL,KEK, CERN, IHEP….)**
**MMF (Moscow)**
**SNS**

**SNS**
CERN SPL
ESS

From P. Ostroumov (2012)

# Linac cost

$$C = C_L L + C_P (P_S + P_B)$$

- Total cost; *L* is the length of linac
- Capital cost per meter $C_L$
- Capital cost per watt of power $C_P$

$$\Delta W = qeEL\cos\varphi$$

- Energy gain

$$P_S = \frac{E^2 L}{Z_{EFF}}$$

- Power loss; *E* includes TTF

$$P_B = \frac{I\Delta W}{eq}$$

- Beam power

From P. Ostroumov (2012)

# Linac cost (cont.)

$$C(E) = \frac{\Delta W}{eq}\left(\frac{C_L}{E\cos\varphi} + \frac{C_P E}{Z_{EFF}\cos\varphi} + C_P I\right)$$

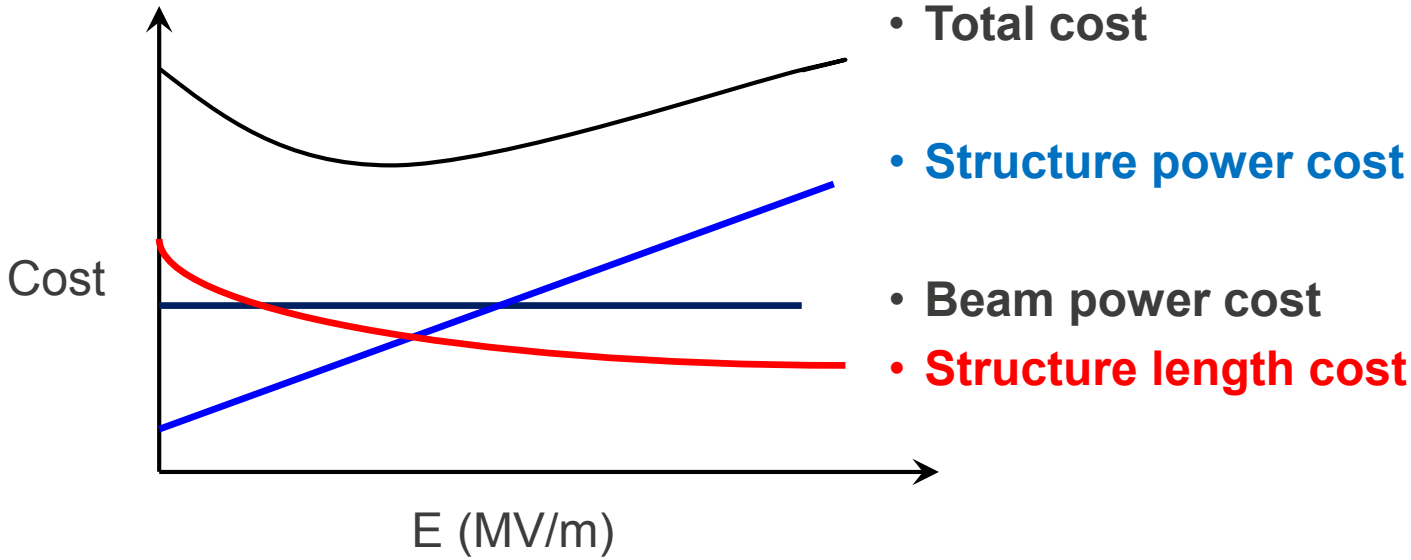


Accelerating field can be limited by breakdowns in resonators

From P. Ostroumov (2012)

# Particle sources

Electron guns: (a) Thermionic cathodes with DC or RF gun
(b) Photo-injectors (photo-cathode with DC or RF gun).

1. Fields in 1.6-cell S-band photo-injector. On-axis field near cathode ~100 MV/m.

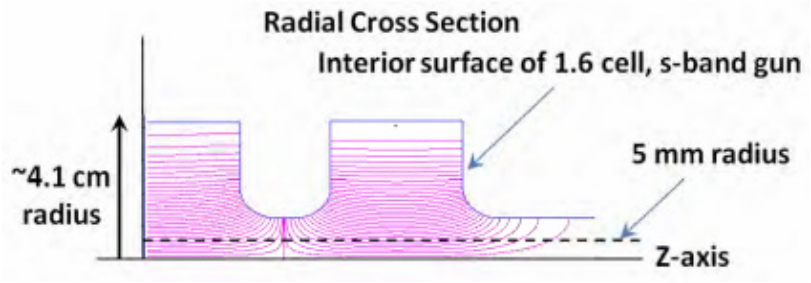


10 nC

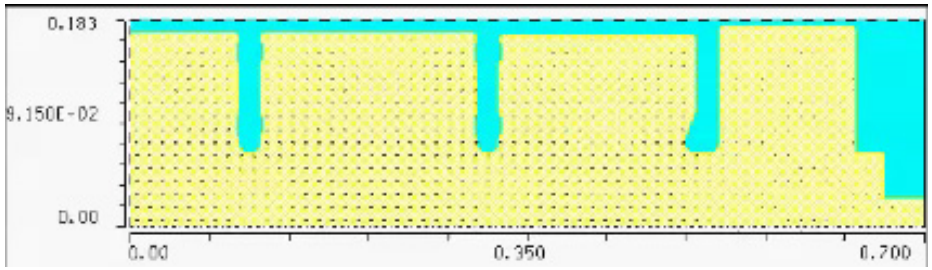


2. LANL CW FEL photo-injector 7-7-5:
2.5 cells, 700 MHz, 1-10 nC/bunch

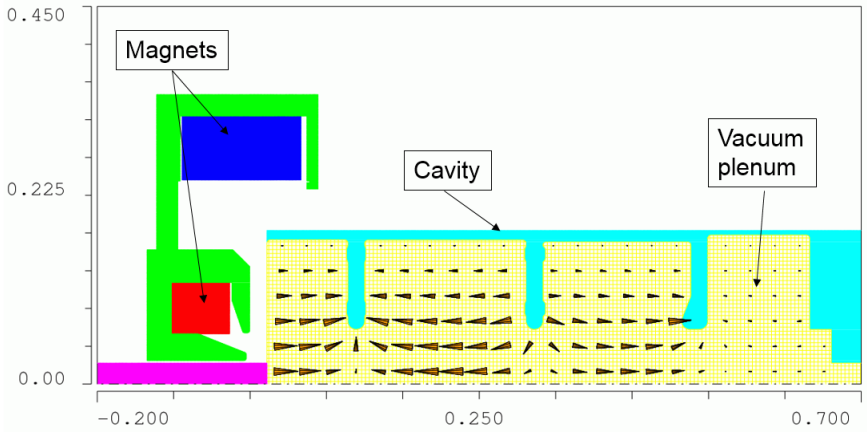


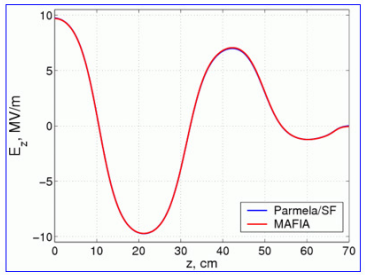


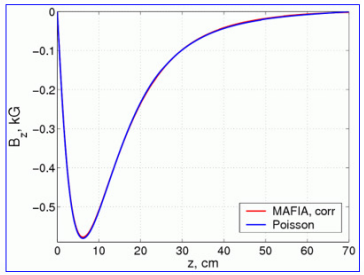


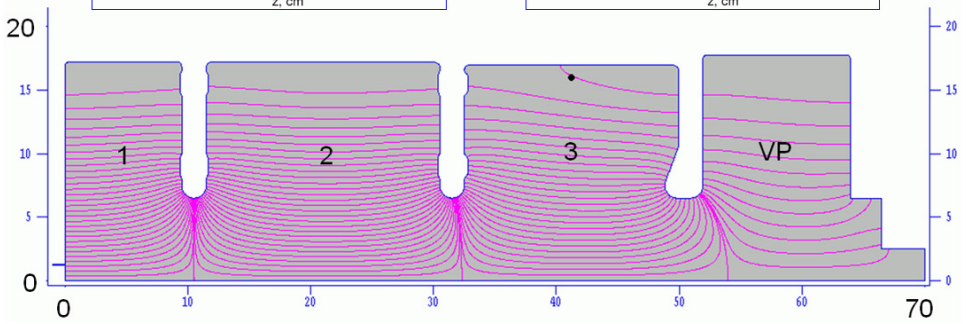

# LANL CW FEL RF photoinjector (2004)

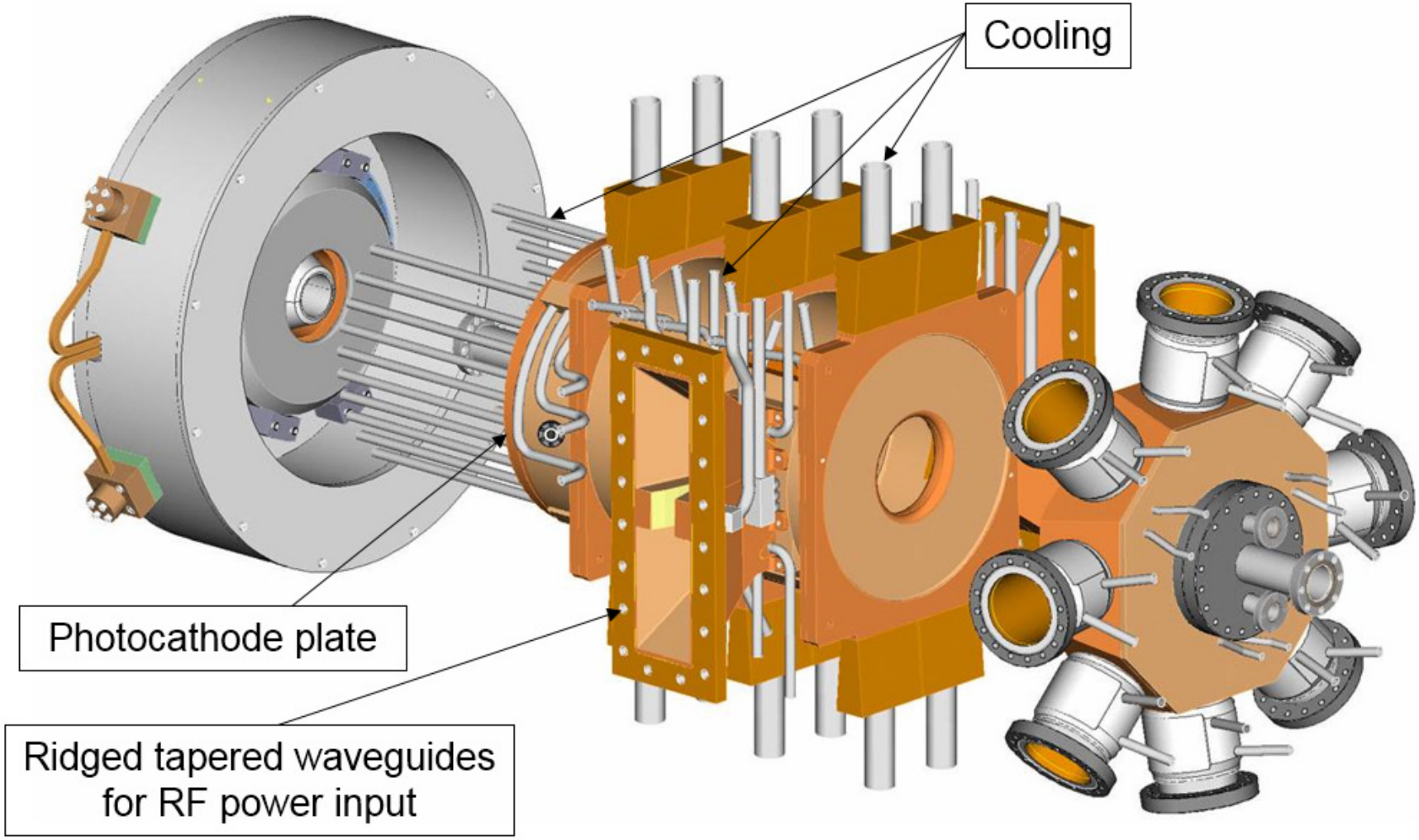


Frequency 700 MHz, 100% duty. Output beam (demo): 100 mA at 2.5 MeV.
RF power deposited in the cavity copper walls ~700 kW.

# Ion sources

"Sourcerers"

Ion source is a device that creates ions, atomic or molecular.

- For protons, hydrogen plasma sources based on gas discharge are used, e.g., duoplasmatron or magnetron-based sources. A combination of electric and magnetic fields creates and contains plasma from a gas flowing through the source, and ion are extracted with an applied external voltage.
- Negative hydrogen ions ($H^-$): hydrogen plasma sources, magnetron-based or more specialized (Penning source), often with added Cs.
- For heavy ions, electron-cyclotron resonance (ECR) sources or electron-beam ion sources (EBIS) are used.

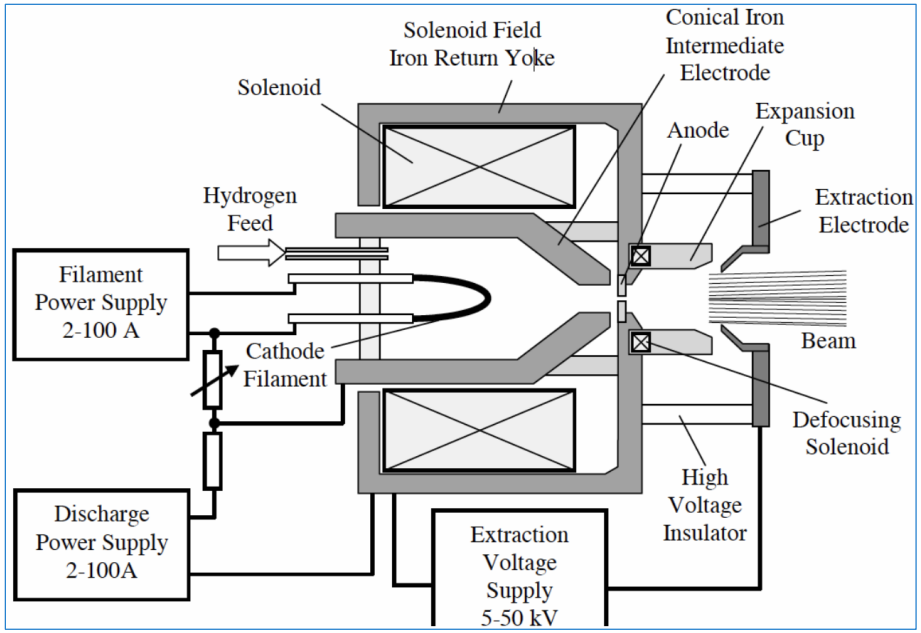


Duoplasmatron scheme and photo (p, LANSCE)

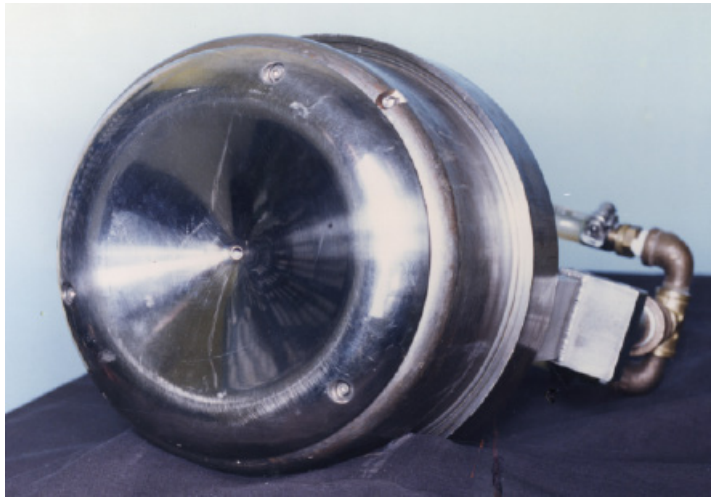

# Example of $H^-$ ion source

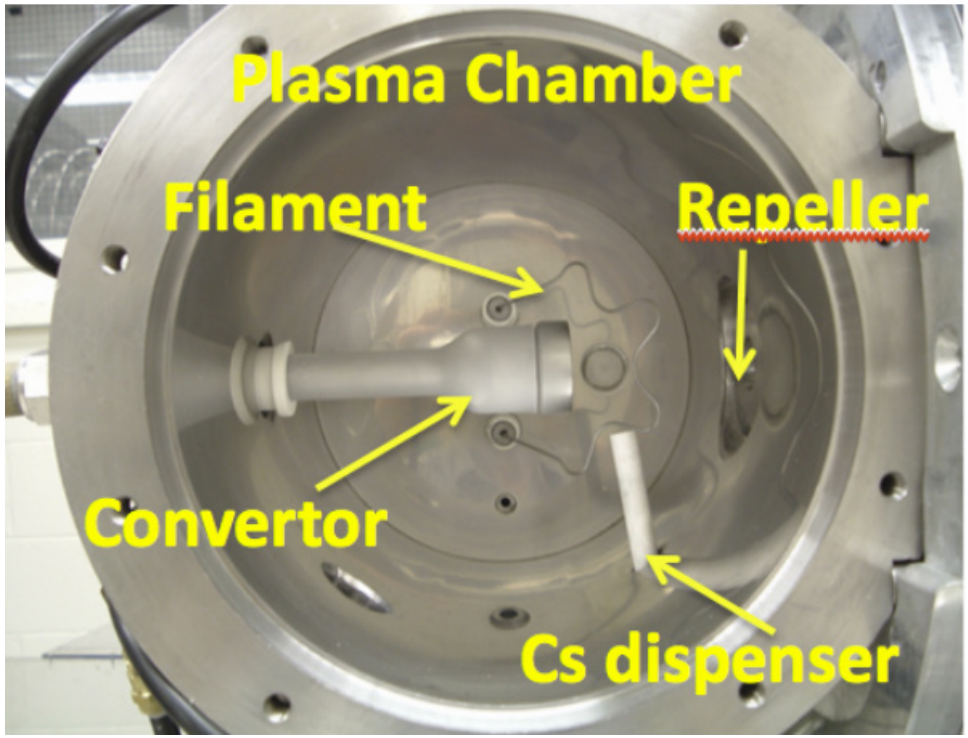


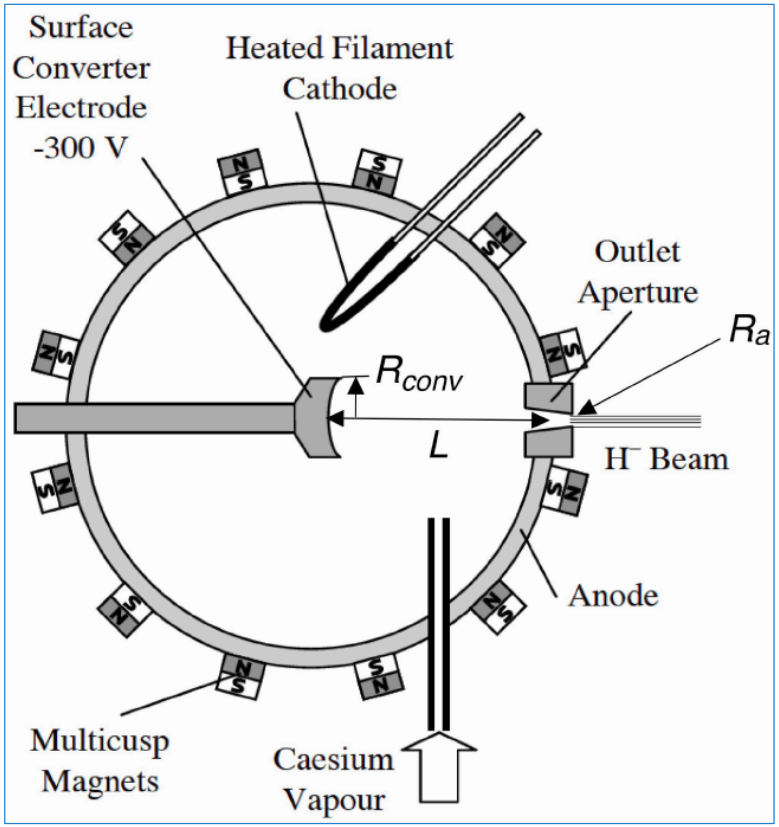


LANSCE multicasp surface converter ion source

Electrons emitted from hot filaments hit the converter surface and produce $H^-$ ions. Cs atoms are deposited on the cold converter to reduce its surface work function. The produced ions are extracted (-300 V), up to 17 mA at 12% duty. The multicasp magnetic field near the chamber walls prevents electrons from escaping to the walls. (Too) Many parameters …

"Sourcerers"

# Low-energy beam transport (LEBT)

SNS $H^-$ ion source and the following electrostatic LEBT (to RFQ, 35 kV)

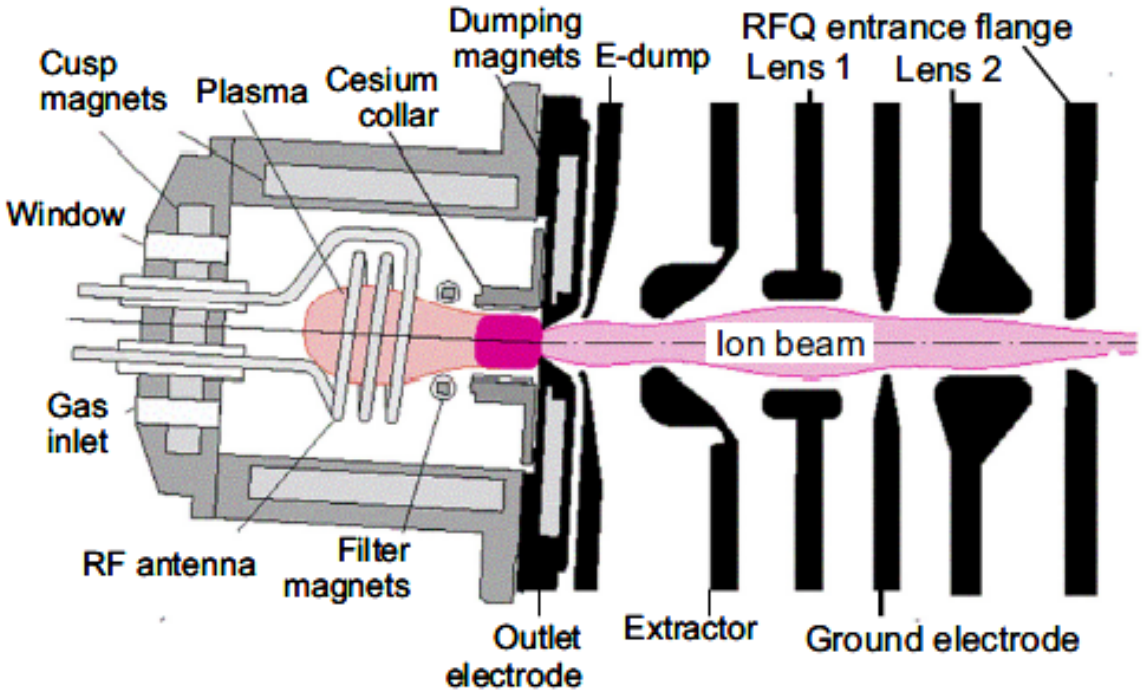


Note RF antenna for heating the plasma. The extracted current up to 40 mA at 6% duty.

LEBTs can electrostatic (short) or magnetostatic (long, with solenoids, usually more flexible). Often LEBTs are used to get rid of unwanted ion species (p, $H^0$, …)

# Radio-Frequency Quadrupole (RFQ) linac

RFQ was invented in 1968 (I. Kapchinsky, V. Teplyakov) and the 1st operational RFQ was built in 1972 (IHEP, Protvino, Russia). The idea was to use asymmetric RF fields to focus particles alternatively in *x* and *y*, plus also accelerate them.

Transverse focusing by RF electric fields is very efficient at *v*<<*c*!

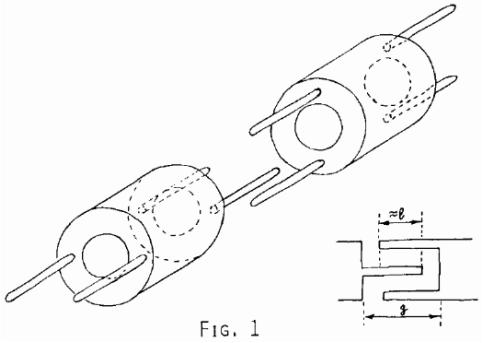

FIG. 1

V. Vladimirsky, 1956

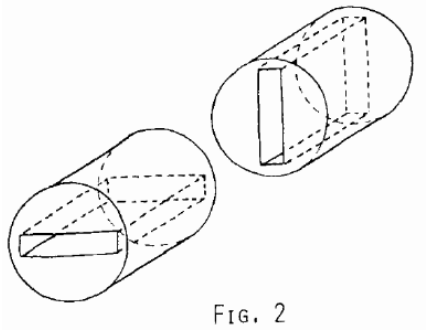
FIG. 2

Teplyakov, Lapostole, 1962

Demo RFQ (IHEP, Protvino, Moscow Region, Russia)
1972
100 – 620 keV, 200 mA, protons
148.5 MHz, 0.0025 % duty
Cu-plated carbon steel cavity, brazed OFE Cu vanes
First operational RFQ, H-mode cavity

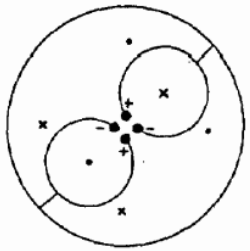
Double-H-Resonator
( 2 · $TE_{110}$ - like)

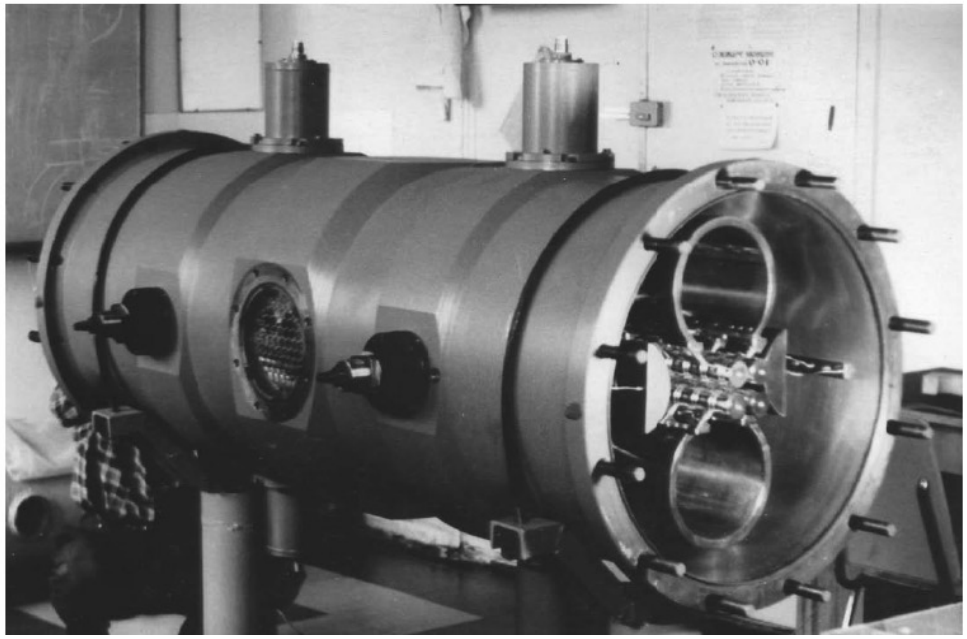

# Radio-Frequency Quadrupole (RFQ) linac

The longitudinal field in RFQ is produced by modulation of electrodes.

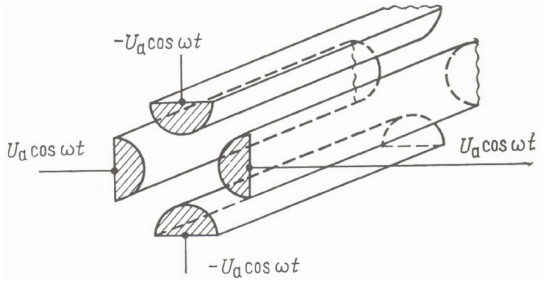


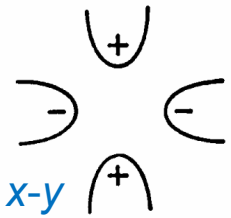


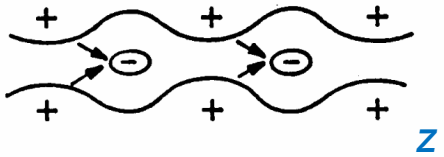


On axis $V$=0 for symmetric $x$-$y$ cross section. Move (+) in: $V$>0; move (-) in: $V$<0. Just keep moving (changing electrode profile – modulation) – it creates longitudinal field ($E_z$).

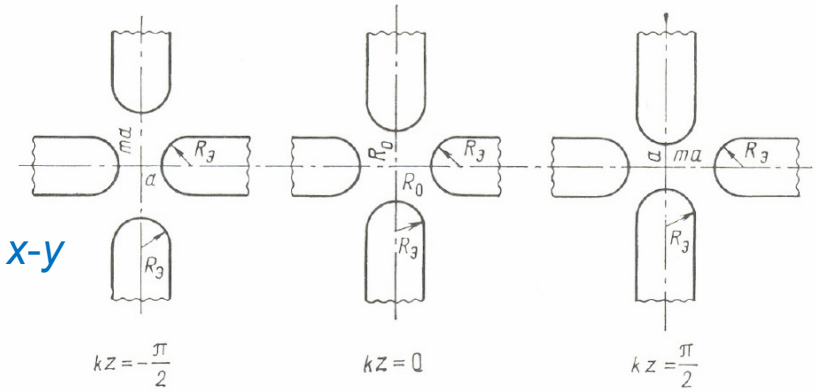


This electrode (vane, rod) modulation can be implemented in various cavities where an appropriate quadrupole mode exists.

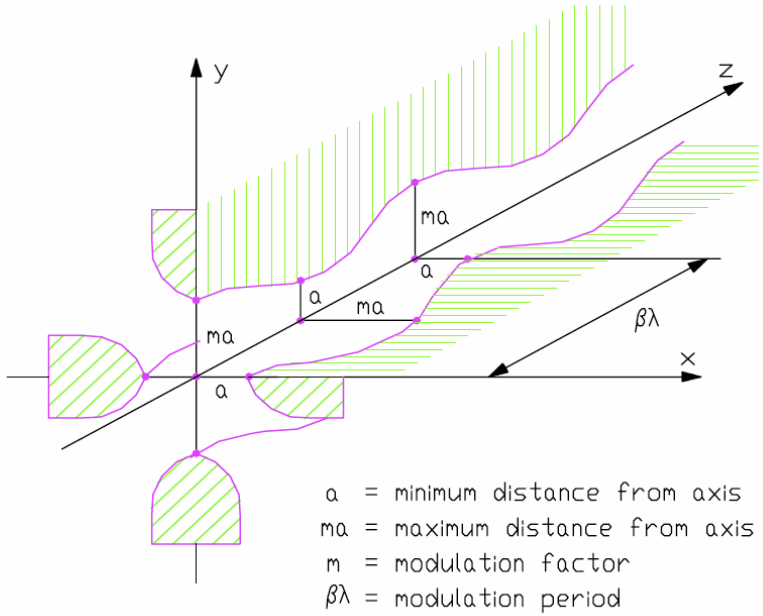

# RFQ: 4-vane cavity

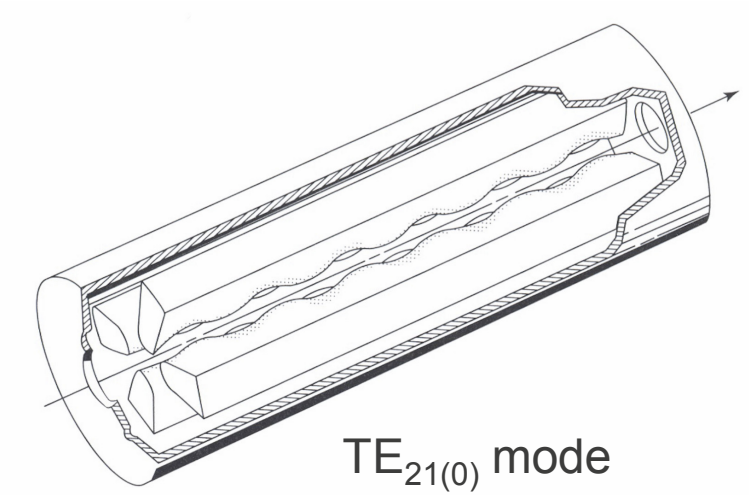


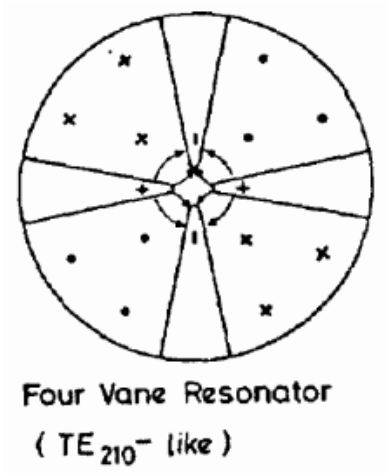


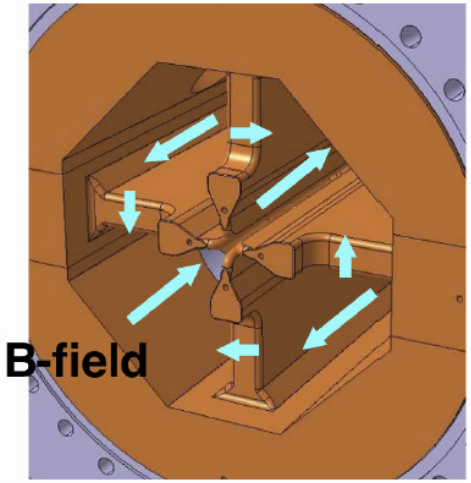


The first 4-vane RFQ was built at LANL in 1980 (telegram to IHEP).

Proof-of-Principle RFQ –1980
30-mA proton beam, 425 MHz
100 keV to 640 keV

Since then the RFQ theory and design tools have been developed (Parmteq).

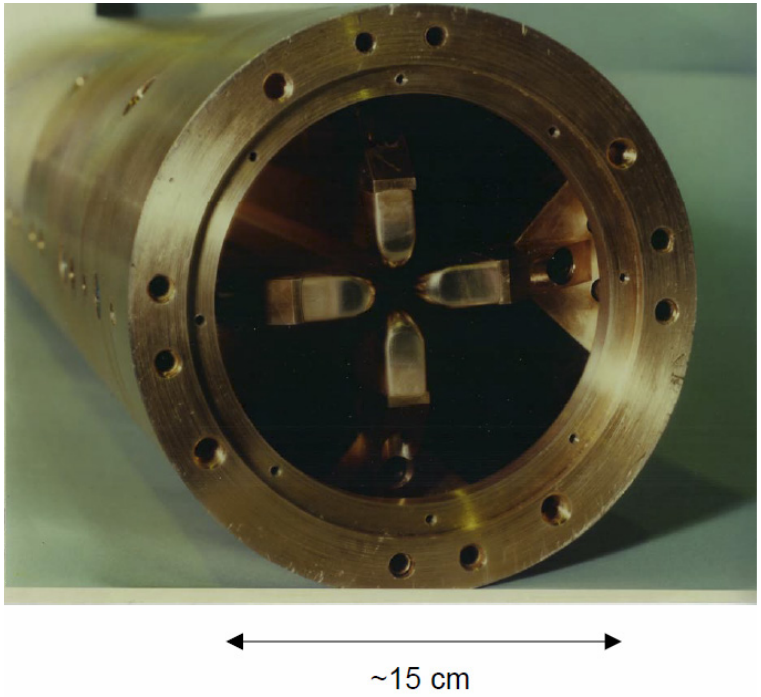

# RFQ sections

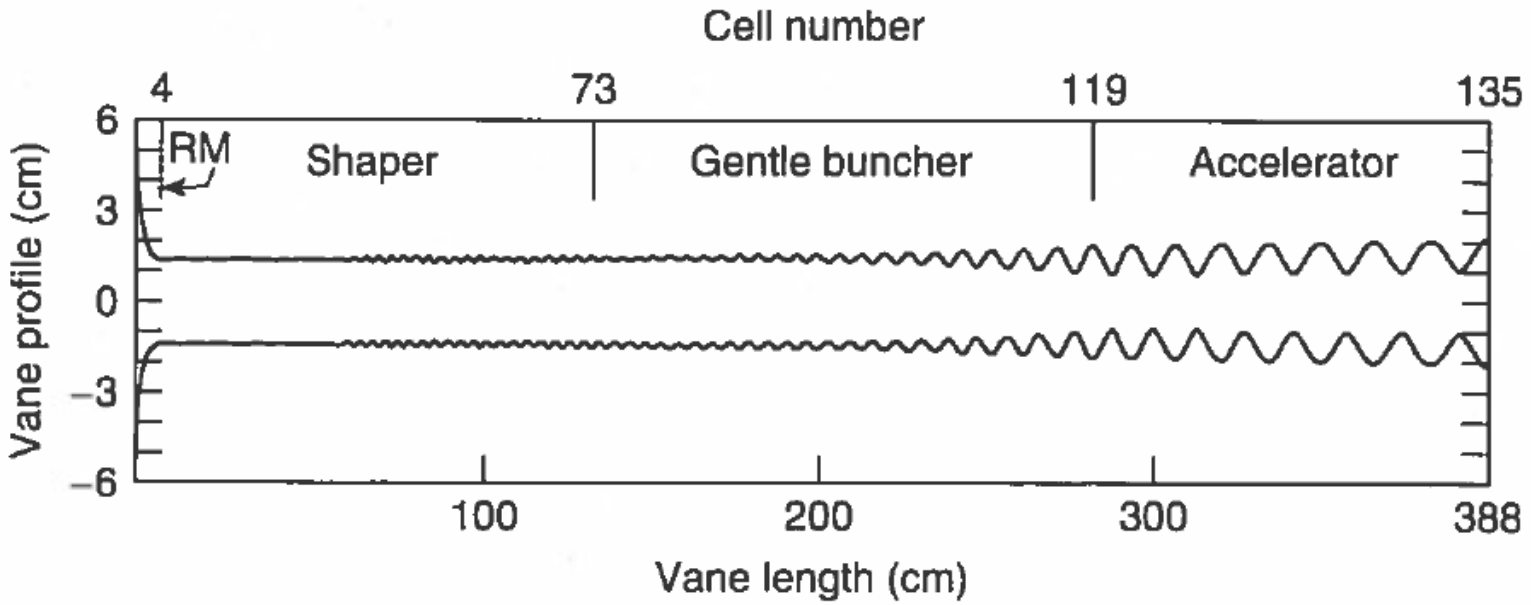


RFQ starts with a short radial matcher (RM), followed by shaper and gentle buncher sections, and ends with an accelerating section (max modulation).

Most of the RFQ length is used to form and bunch the beam; only near the end the beam is accelerated. The synchronous phase changes from -90° to -40° / -20° along the length. The cell length increases with $\beta$ as $L_c = \beta\lambda/2$.

# Many more 4-vane RFQs

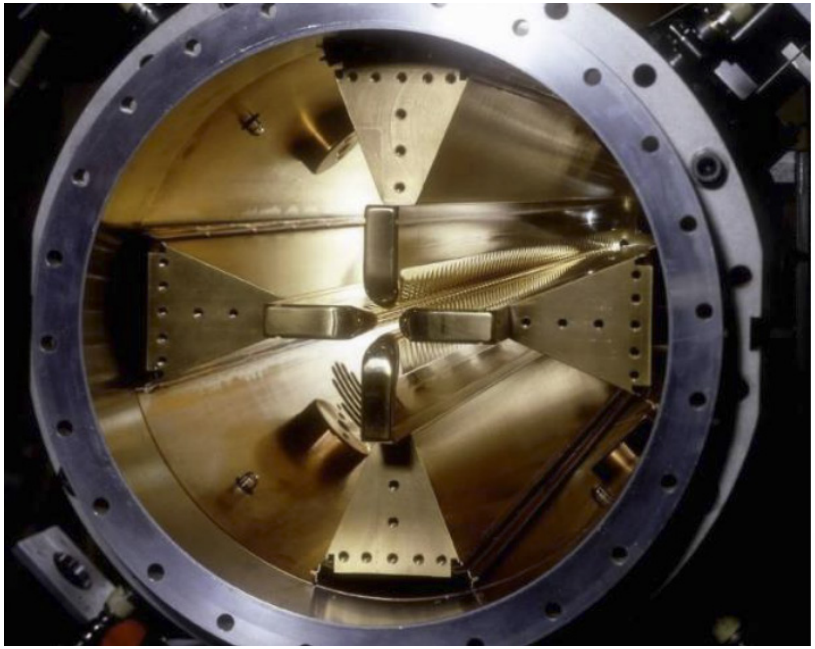

CERN RFQ1 (1983)
202 MHz, 80 mA protons
to 520 KeV

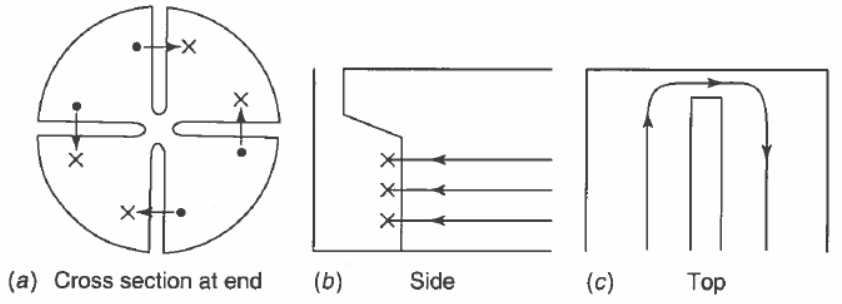


CERN RFQ for Linac 4 (2013)
352 MHz, 70 mA $H^-$, 45 keV to 3 MeV
length 3 m, inter-vane voltage V=78 kV
beam capture 95%

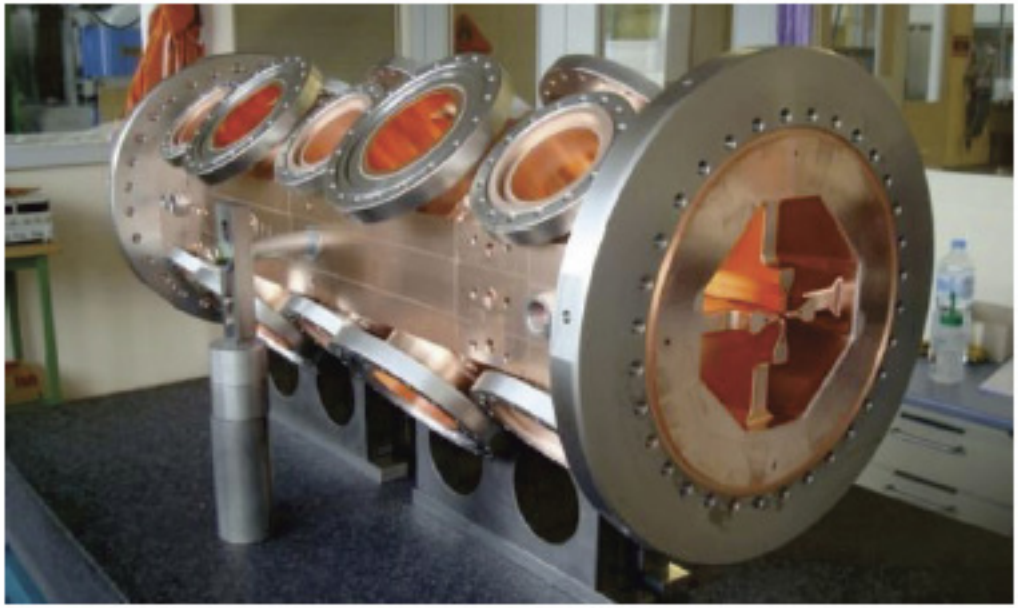

# World-record RFQ

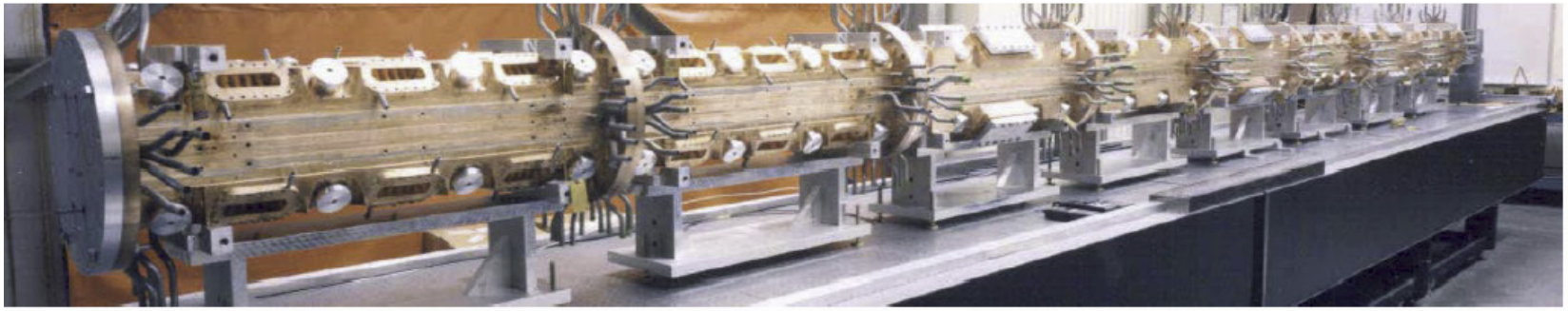

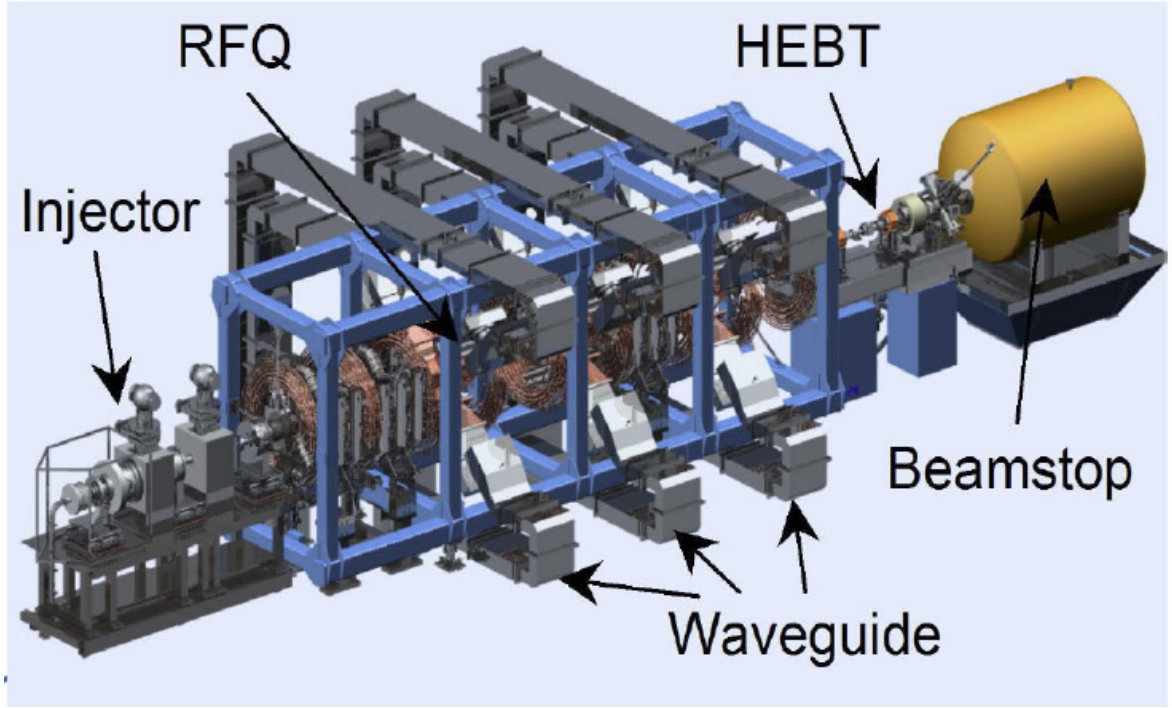


LEDA RFQ (1999)

Most powerful RFQ was 350-MHz 8-m long CW RFQ that accelerated a 100-mA proton beam at Los Alamos (LEDA) from 75-keV to 6.7-MeV

Beam power 670 kW!

# 4-vane RFQ variations

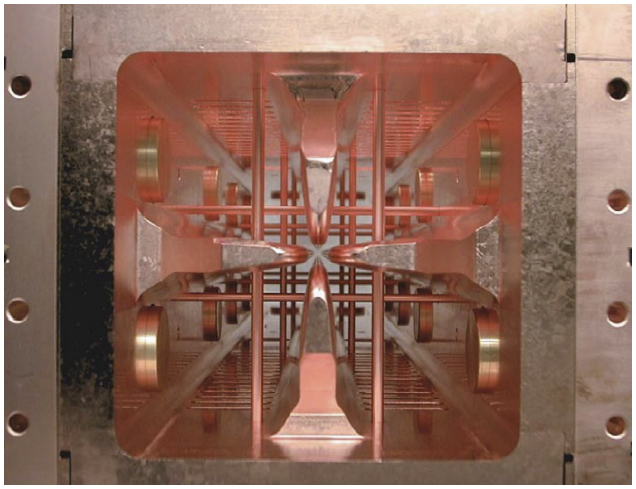

SNS 4-vane RFQ with $\pi$-mode stabilizers. Total length is 3.72 m, 4 modules. 402.5 MHz, 40 mA $H^-$, 65 keV to 2.5 MeV

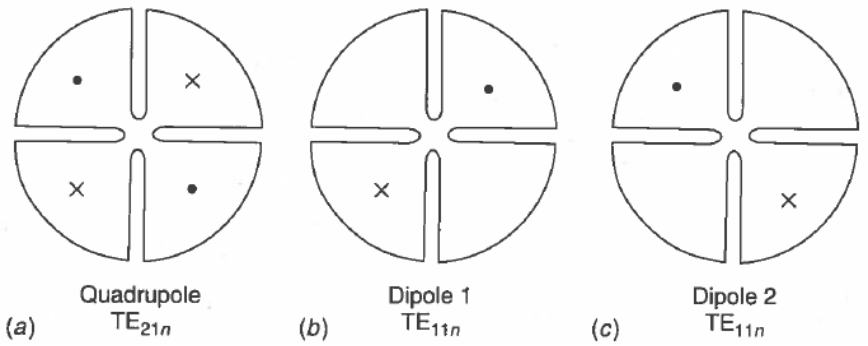


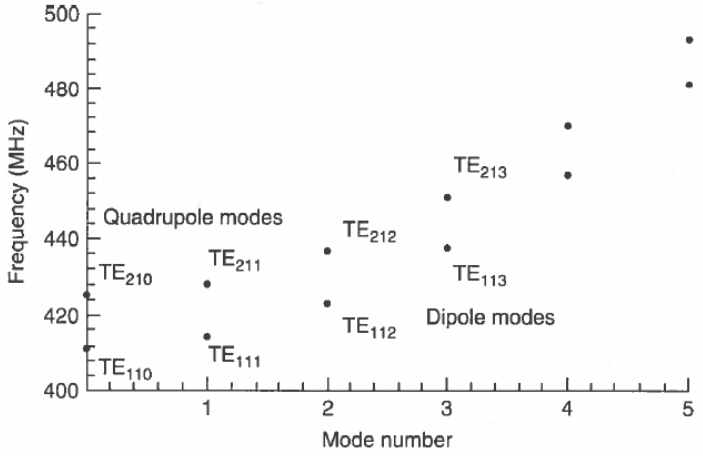


The main design problem in 4-vane RFQs is to get rid of unwanted dipole modes with frequencies close to the operating quadrupole mode.

# 4-vane RFQ cavity

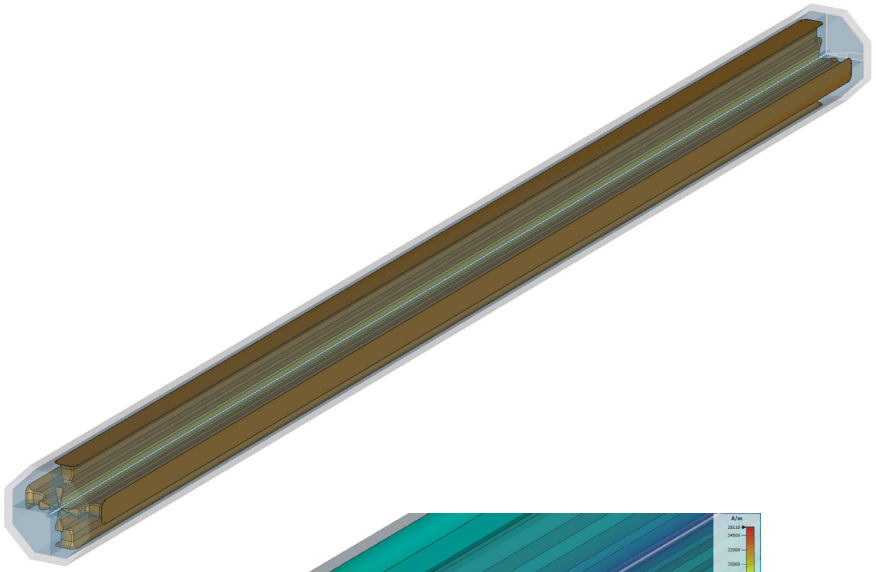

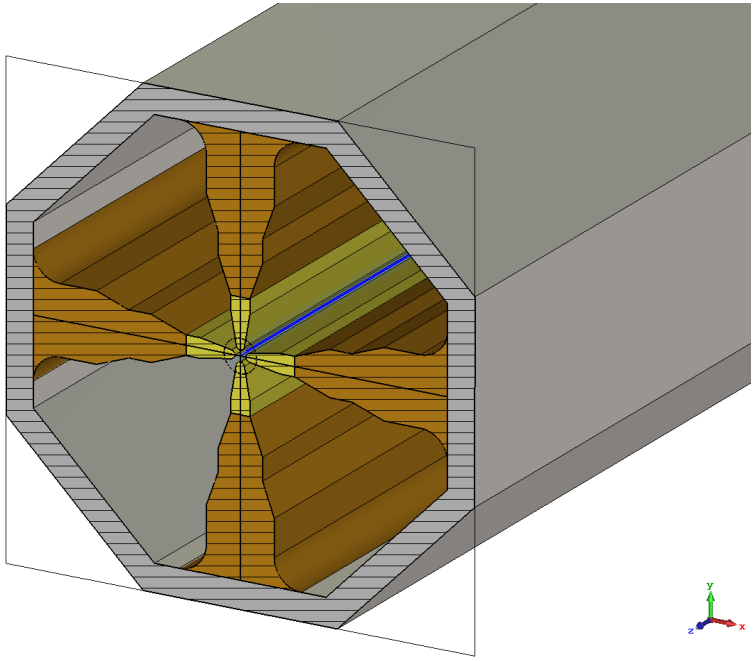

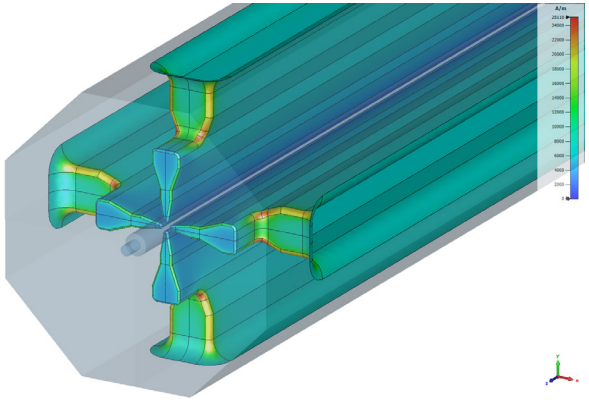

4-vane RFQ for 425 MHz, 55 keV to 2 MeV. Undercuts on the vane edges are made for magnetic fields to turn around the vanes without strong increase.

# Fields in 4-vane RFQ cavity - slice

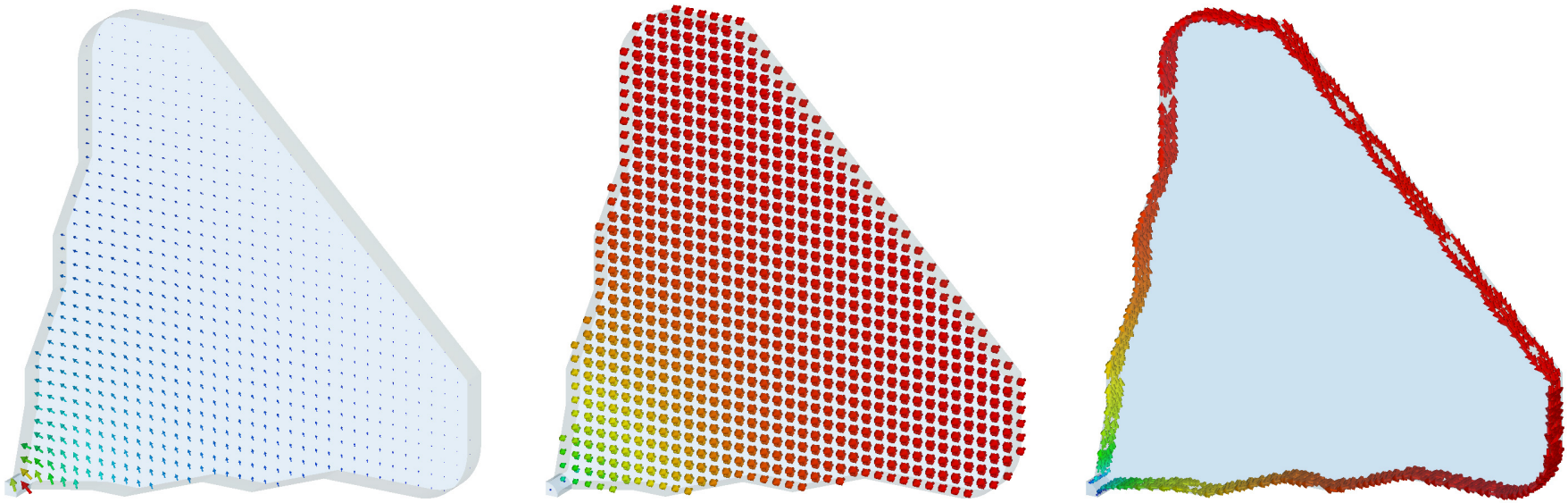

Electric field (left), magnetic field (center), and surface current (right) in a slice (one quarter) of the RFQ cross section.

# Fields in 4-vane RFQ cavity

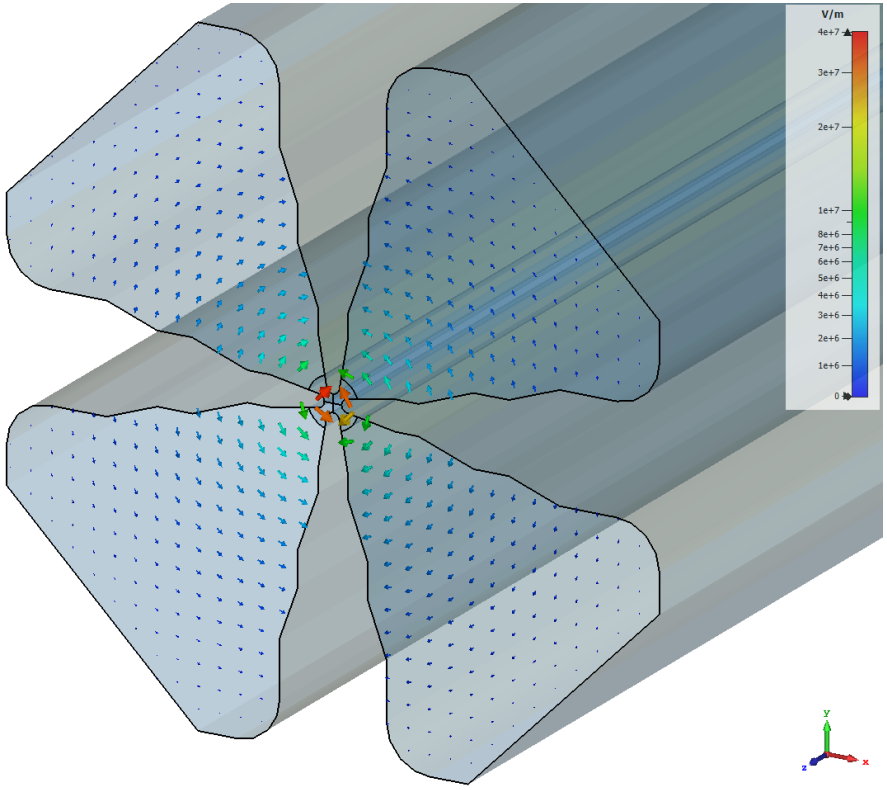


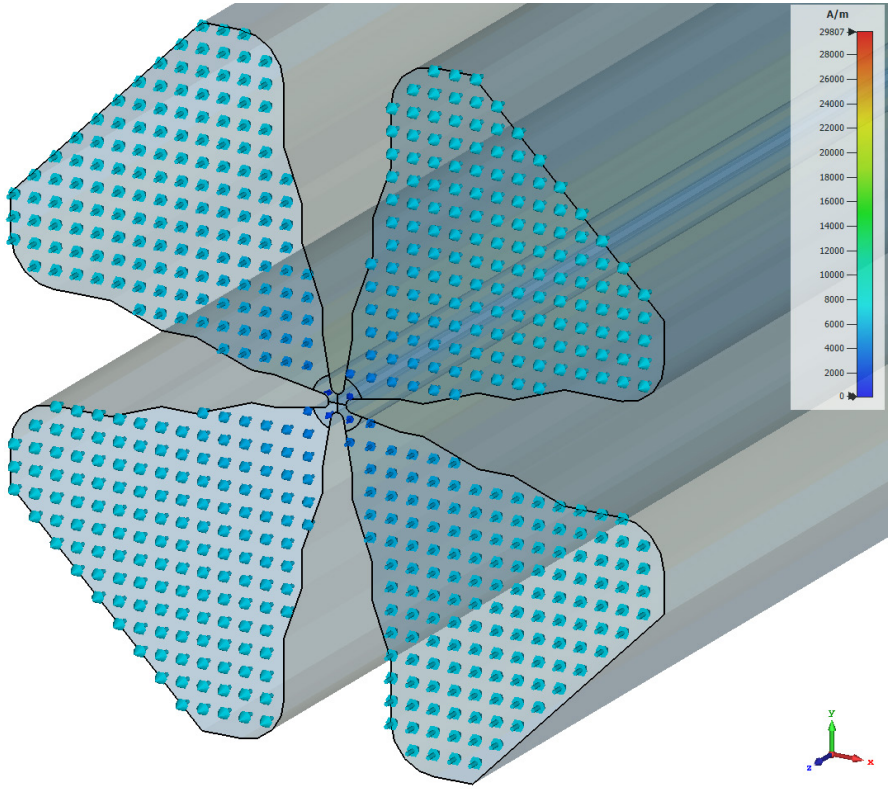


Electric (left) and magnetic field (right) in an RFQ cross section

# 4-rod RFQs

4-rod RFQ was proposed by A. Schempp in 1985. Four rods have profile modulations. The mode frequency in each structure period (between two supports) depends on L, C, not on the cavity shape.

No problems with mode separation, less sensitive to mechanical errors. Usually 4-rod RFQs are used at lower frequencies, < 100 MHz, for heavy ions, but some are designed for > 200 MHz.

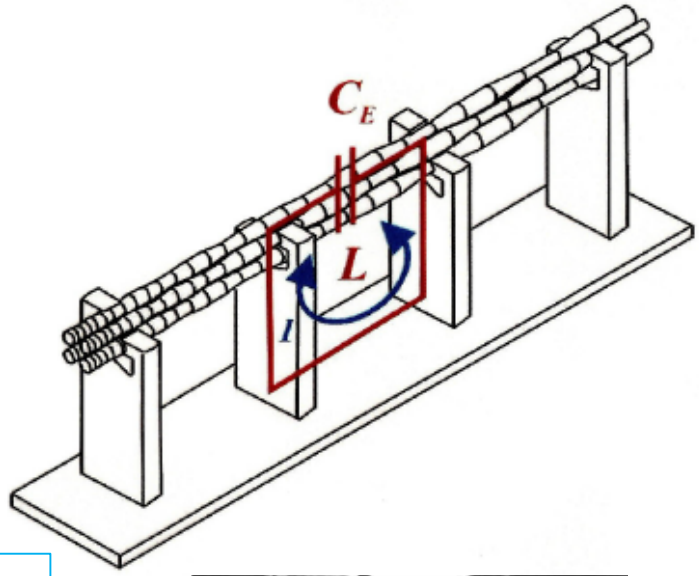


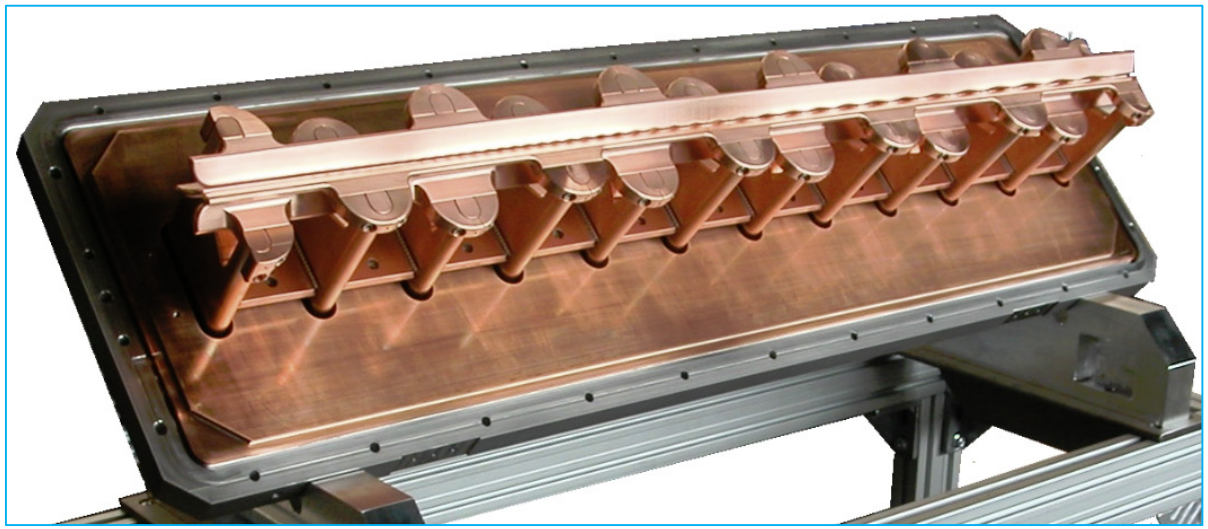

FNAL 201.25-MHz RFQ (2011). Low duty, 1.2-m long. 60 mA $H^-$, 35 keV to 750 keV. Moveable tuning plates, V-shaped cooling channels in support stems.

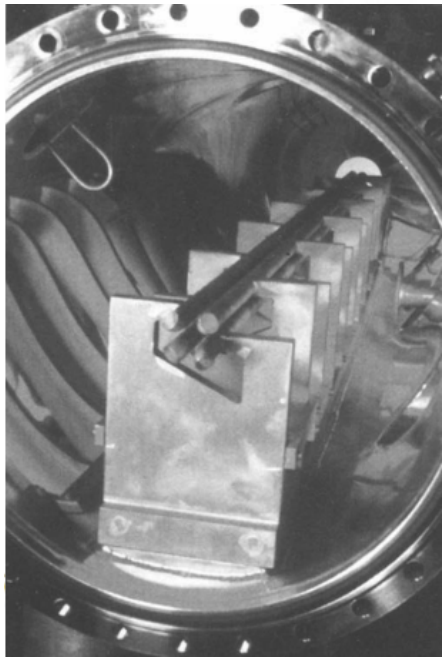

# FNAL 4-rod RFQ

Problems with final energy – 710 keV instead of 750 keV.

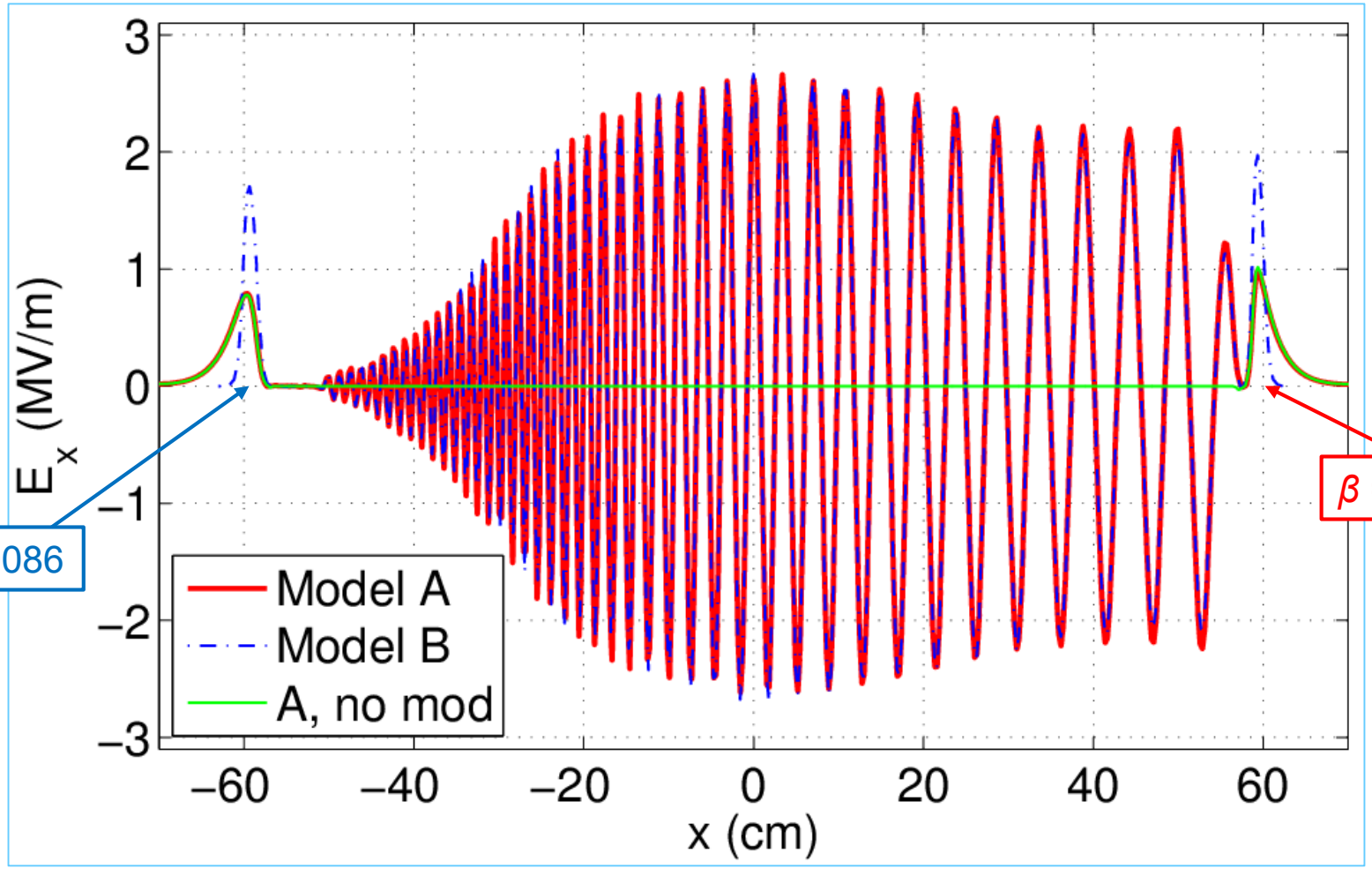


CST MWS calculated on-axis longitudinal field: Model A – wide beam pipes, B – narrow ones. The end-gap fields are not predicted by RFQ design codes; can change beam energy.

# CST Particle Studio simulations for FNAL RFQ (Model A)

Particle Studio uses RF fields computed in MWS Studio

Color indicates particle energy change

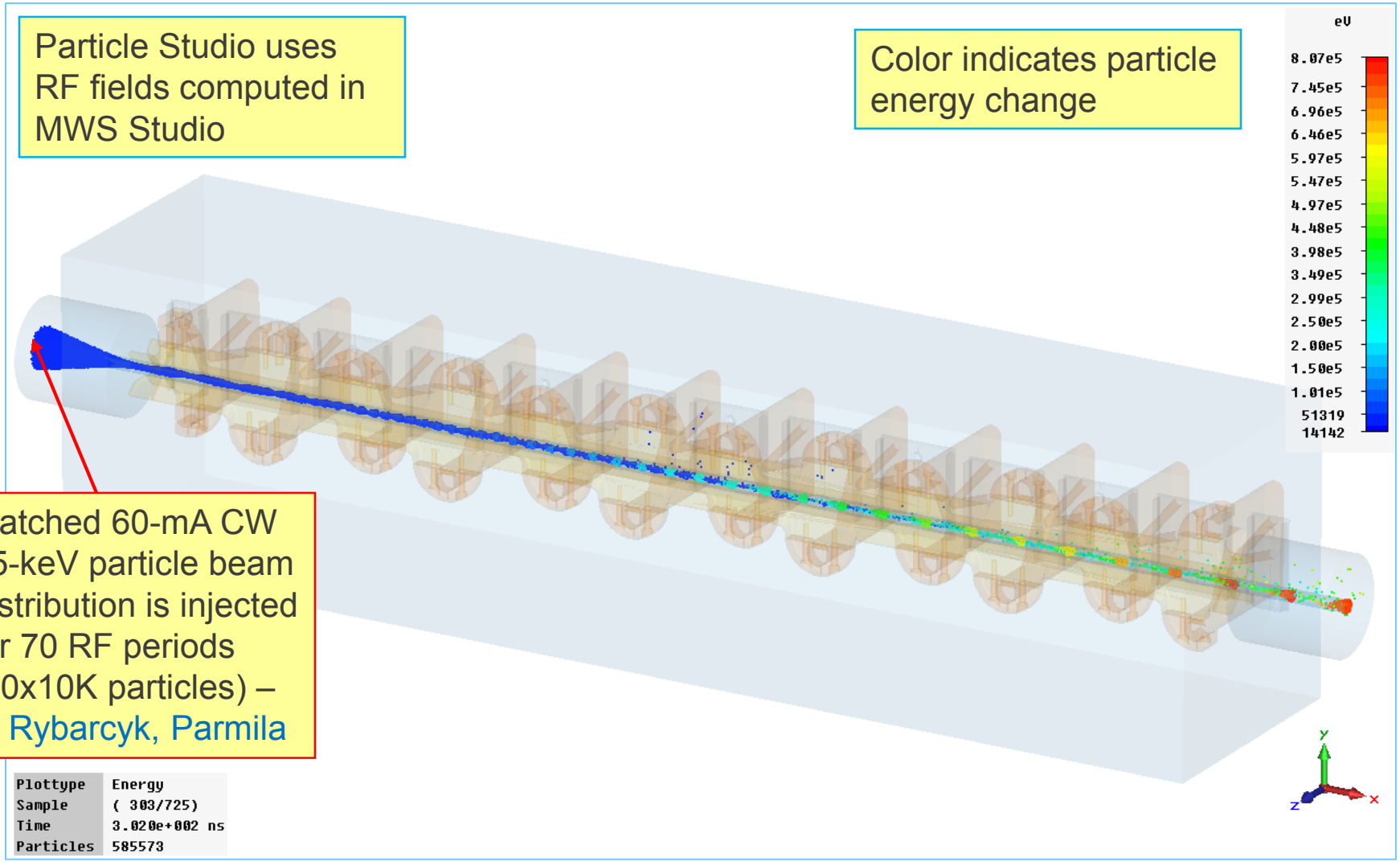


Matched 60-mA CW 35-keV particle beam distribution is injected for 70 RF periods (70x10K particles) – L. Rybarcyk, Parmila

3-D particle monitor: particles in the RFQ cavity at $t$ = 302 ns

# RFQ – just remove some unneeded parts

## FNAL RFQ, June 28, 2012: energy fixed

### Energy after end plate removal

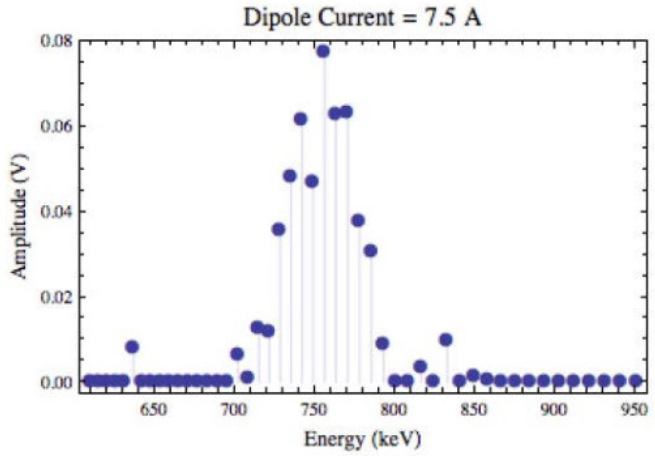


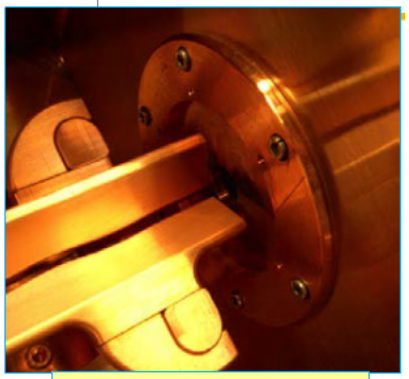

The end plate before removal

Energy is 756.5 ± 0.5 keV @ 170 forward, 3 kW reflected.

Energy error is fixed!!!!



It was some useful experience.

# LANL 4-rod RFQ (2014)

201.25-MHz 4-rod RFQ:

- 35 mA $H^-$, 35 keV to 750 keV
- duty up to 15%, 1.75-m long
- inter-vane voltage 50 kV
- cooling channels in both stems and rods

Designed by LANL & IAP (Frankfurt)

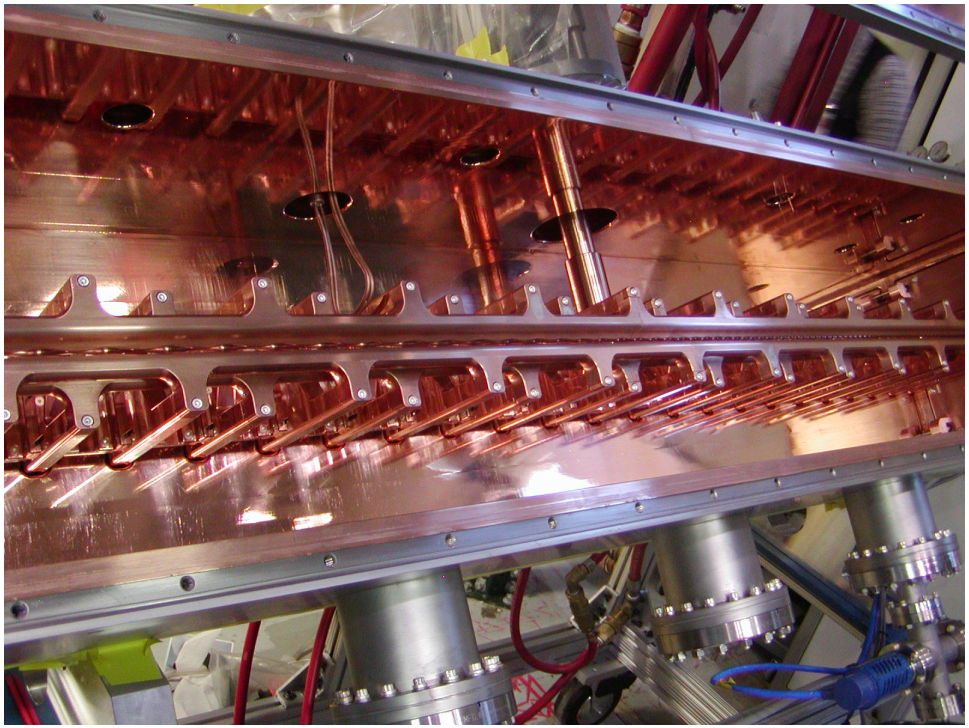

Manufactured by Kress GmbH (2015)

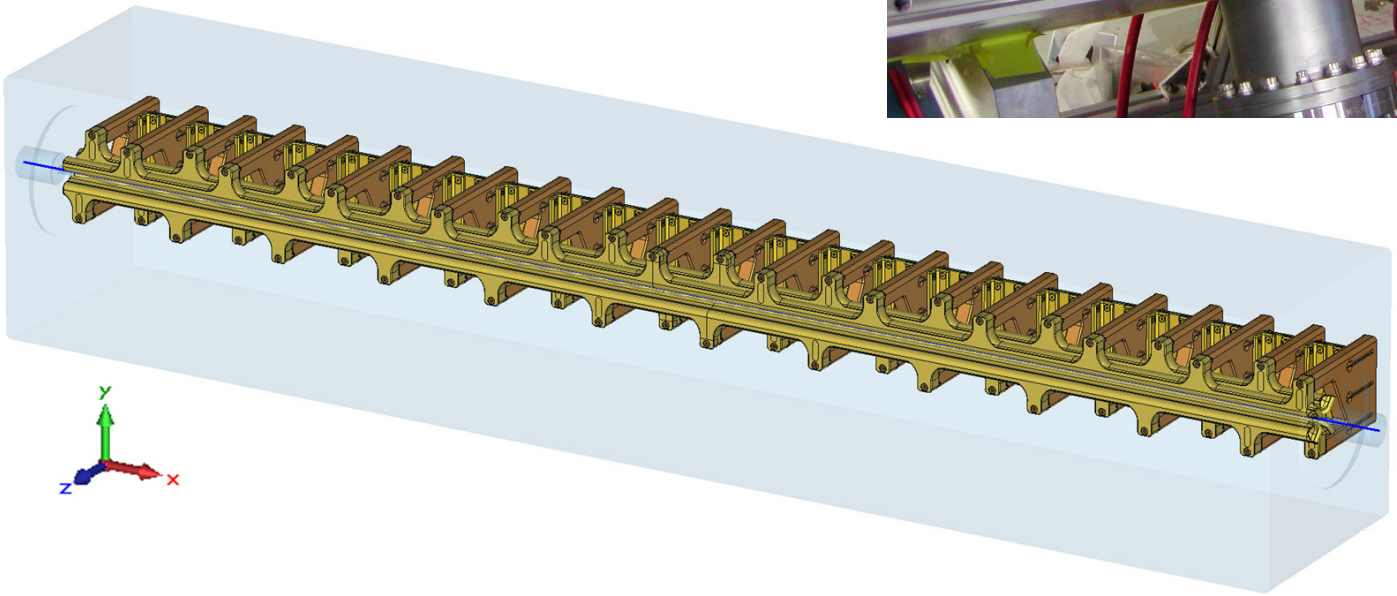

# LANL 4-rod RFQ Particle Studio Simulations

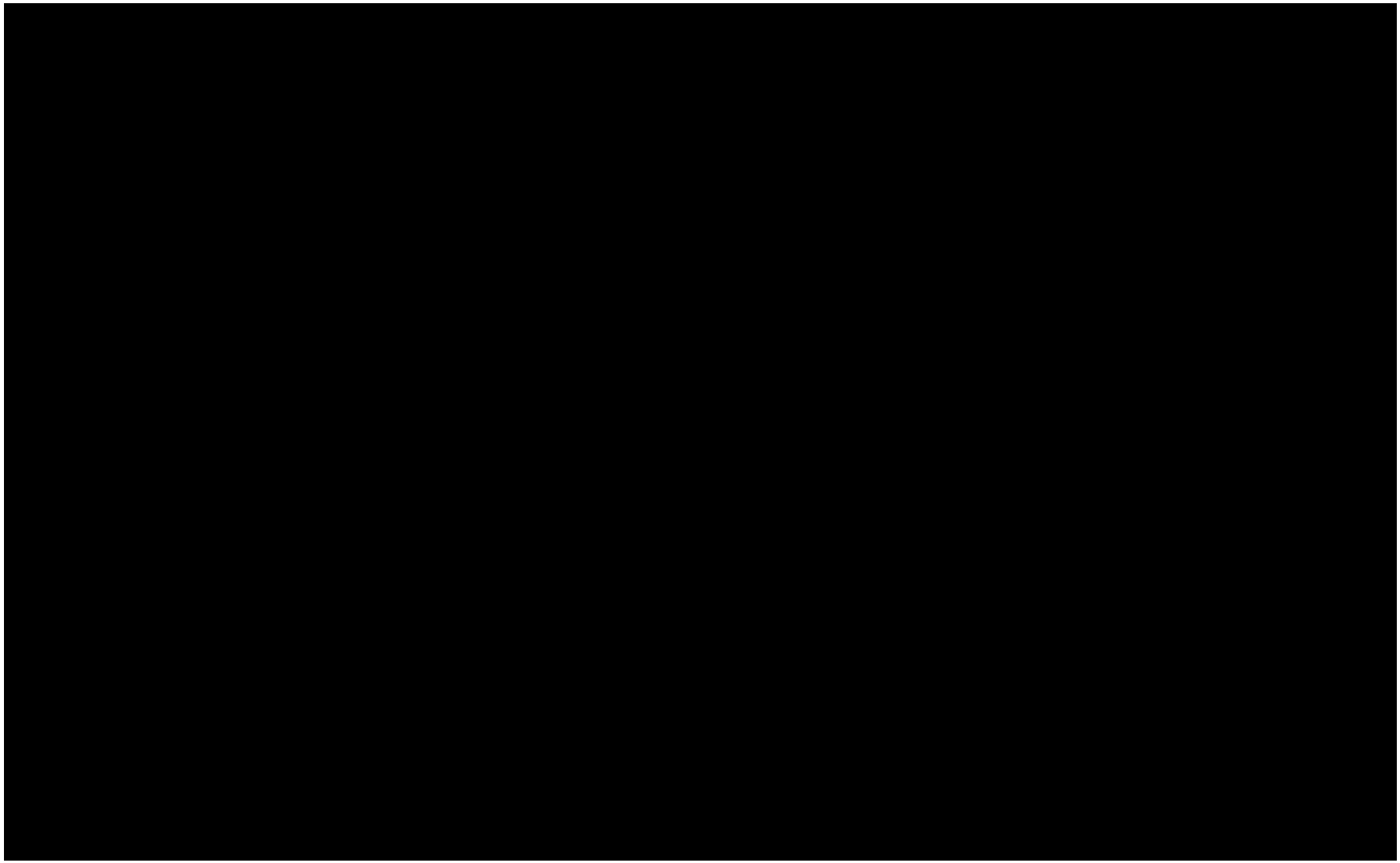

100 RF periods injected. Beam current 35 mA, inter-vane voltage 60 kV.

# Drift-Tube Linac (DTL)

Alvarez DTL structure (1946):

- $TM_{010}$-like mode ($E_z$, $E_r$, $B_\theta$)
- DTs hide the beam bunches during the decelerating phase of electric field
- cell length $L_c=\beta\lambda$
- long cavities (tanks) are more efficient
- field stabilization by post-couplers in long tanks

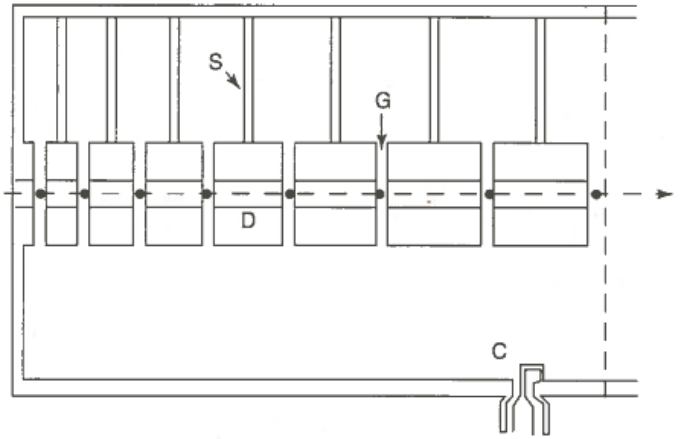


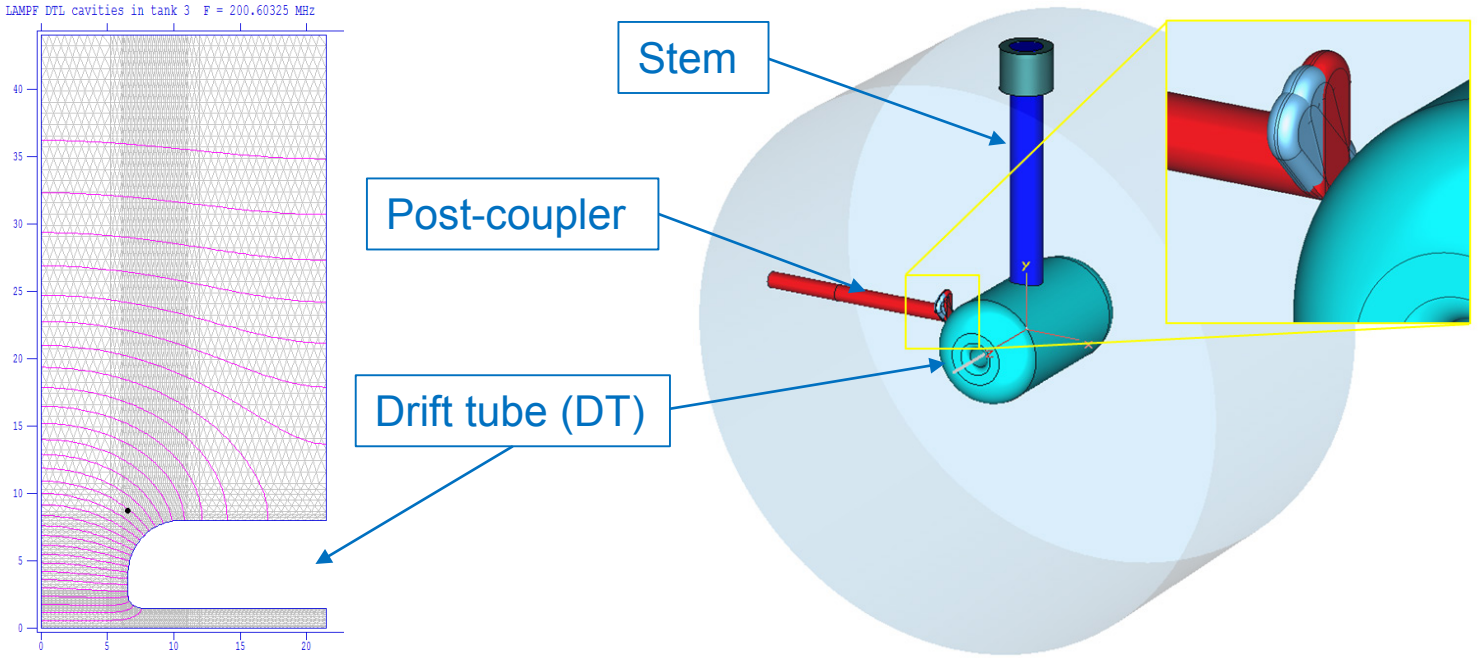


Electric field lines (Superfish, left) and CST model of cell 98 (1st in T3) of the LANSCE DTL.

# LANSCE DTL (1968)

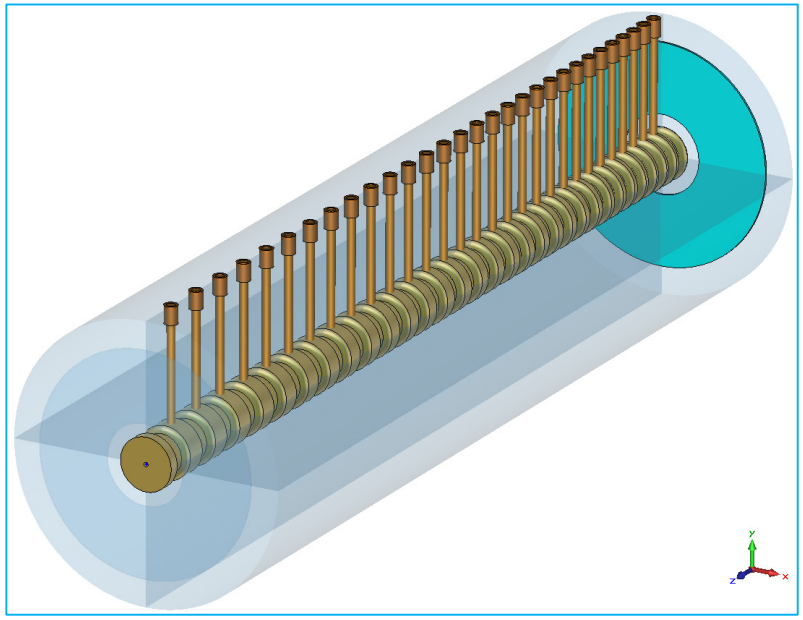

CST model of Tank 1

Usually the average longitudinal field $E_0$ is constant (flat) along the tank length but in T1 it is ramped (increasing). Tilt tuners.

**Table 4.1** DTL parameters for the LANSCE proton accelerator.

| | Tank 1 | Tank 2 | Tank 3 | Tank 4 |
|---|---|---|---|---|
| Cell number | 1 to 31 | 32 to 59 60 to 97 | 98 to 135 | 136 to 165 |
| Energy in (MeV) $\beta$ | 0.75 0.04 | 5.39 0.107 | 41.33 | 72.72 |
| Energy out (MeV) $\beta$ | 5.39 | 41.33 0.287 | 72.72 0.37 | 100.00 0.43 |
| Energy gain (MeV) | 4.64 | 35.94 | 31.39 | 27.28 |
| Tank length (cm) | 326.0 | 1968.8 | 1875.0 | 1792.0 |
| Tank diameter (cm) | 94.0 | 90.0 | 88.0 | 88.0 |
| Drift-tube diameter (cm) | 18.0 | 16.0 | 16.0 | 16.0 |
| Drift-tube corner radius (cm) | 2.0 | 4.0 | 4.0 | 4.0 |
| Bore radius (cm) | 0.75 | 1.0 1.5 | 1.5 | 1.5 |
| Bore corner radius (cm) | 0.5 | 1.0 | 1.0 | 1.0 |
| $g/L$ | 0.21–0.27 | 0.16–0.32 | 0.30–0.37 | 0.37–0.41 |
| Number of cells | 31 | 66 | 38 | 30 |
| Number of quads | 32 | 29 38 | 20 | 16 |
| Quad gradient (kG/cm) | 8.34–2.46 | 2.44–1.89 1.01–0.87 | 0.90–0.84 | 0.84–0.83 |
| Quad length (cm) | 2.62–7.88 | 7.88 16.29 | 16.29 | 16.29 |
| $E_0$ (MV/m) | 1.60–2.30 | 2.40 | 2.40 | 2.50 |
| $\phi_s$ (°) | −26 | −26 | −26 | −26 |
| Power (MW) | 0.305 | 2.697 | 2.745 | 2.674 |
| Intertank space (cm) | 15.90 | 85.62 | 110.95 | – |
| Transit-time factor, $T$ | 0.72–0.84 | 0.87–0.80 | 0.82–0.74 | 0.74–0.68 |
| Mean $ZT^2$ (MΩ/m) | 26.8 | 30.1 | 23.7 | 19.2 |

Total length including intertank spaces = 61.7 m

The best efficiency (higher effective shunt impedance) for DTL is achieved in the beam velocity range $\beta$ = 0.1-0.3. At LANSCE it is used for wider range, $\beta$ = 0.04-0.43.

# LANSCE DTL tank models

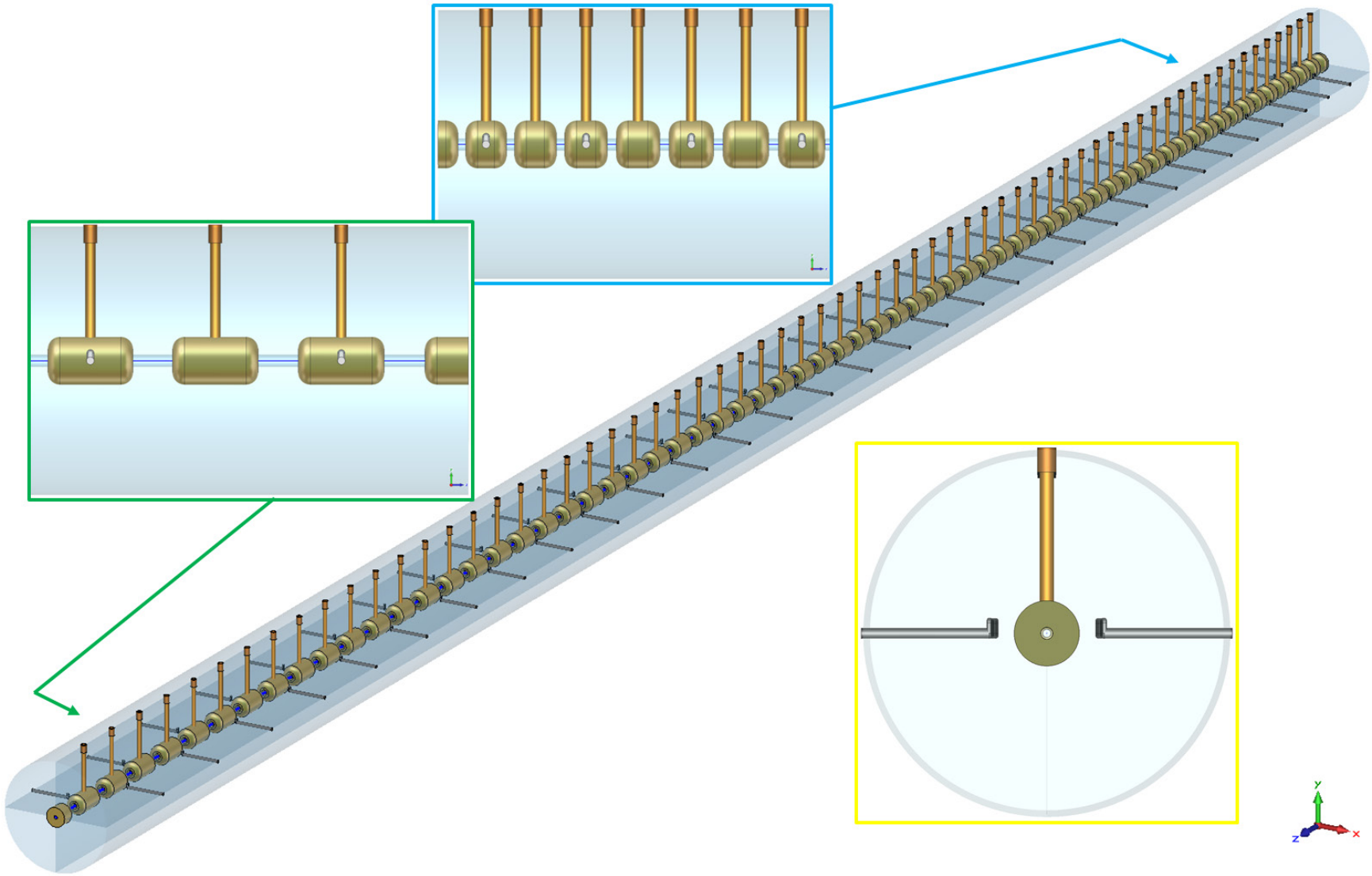

CST model of the LANSCE DTL tank 2: 66 cells, 19.68-m long, $\beta$ = 0.107-0.287

# Fields in DTL tanks

Electric field arrows (MWS norm.) in *x* & *y*-planes near the entrance (right) and exit (bottom) of DTL tank 2.

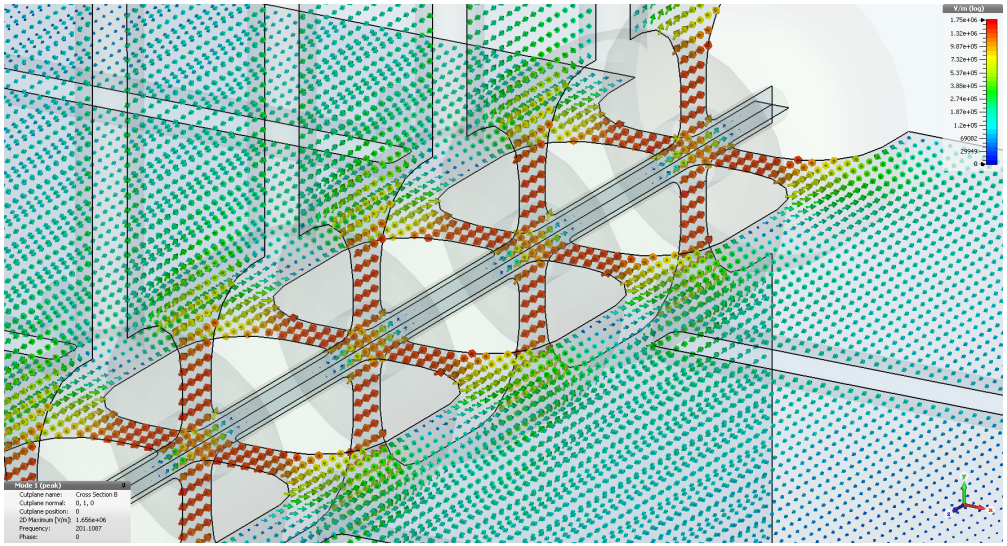

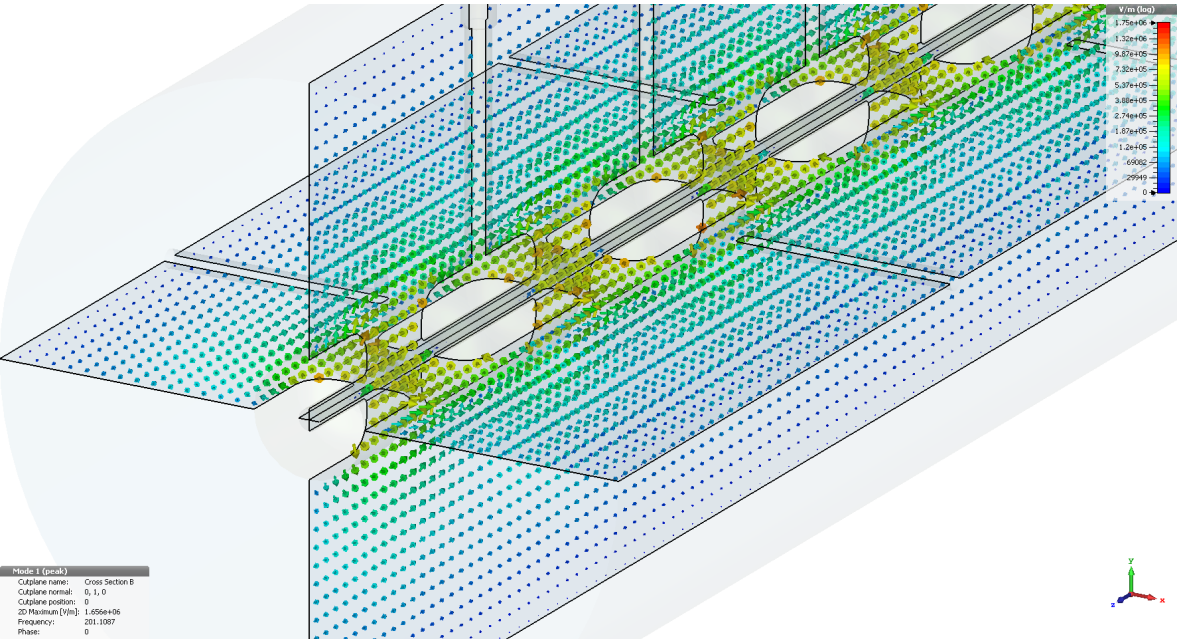

Magnetic fields of quadrupoles near the entrance of DTL tank 1 (imported in PS).

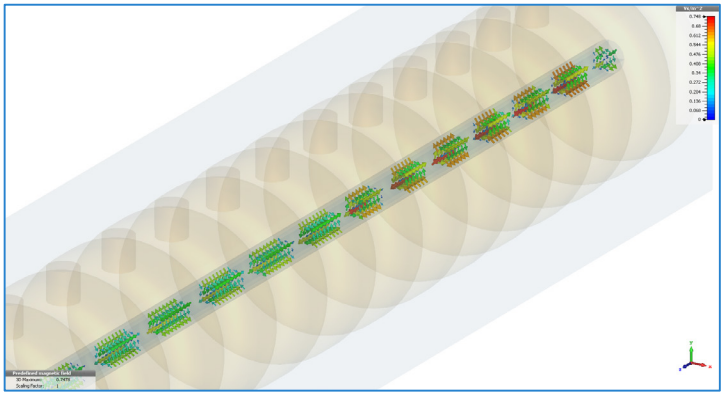

# DTL – PS simulations in LANSCE DTL tanks

Particle Studio simulations of 10 RF periods (10x10K) of 18-mA proton beam injected into DTL tank 1. Transmission 85% (80.6% in bunches, 4.4% in the tail).

# DTL – PS simulations in LANSCE DTL tanks

Particle Studio simulations of 10 RF periods (10x10K) of 18-mA proton beam injected into DTL tank 1 – end-tank view. Transmission 85% (bunches 80.6%, tail 4.4%).

# DTL cavities: tuning

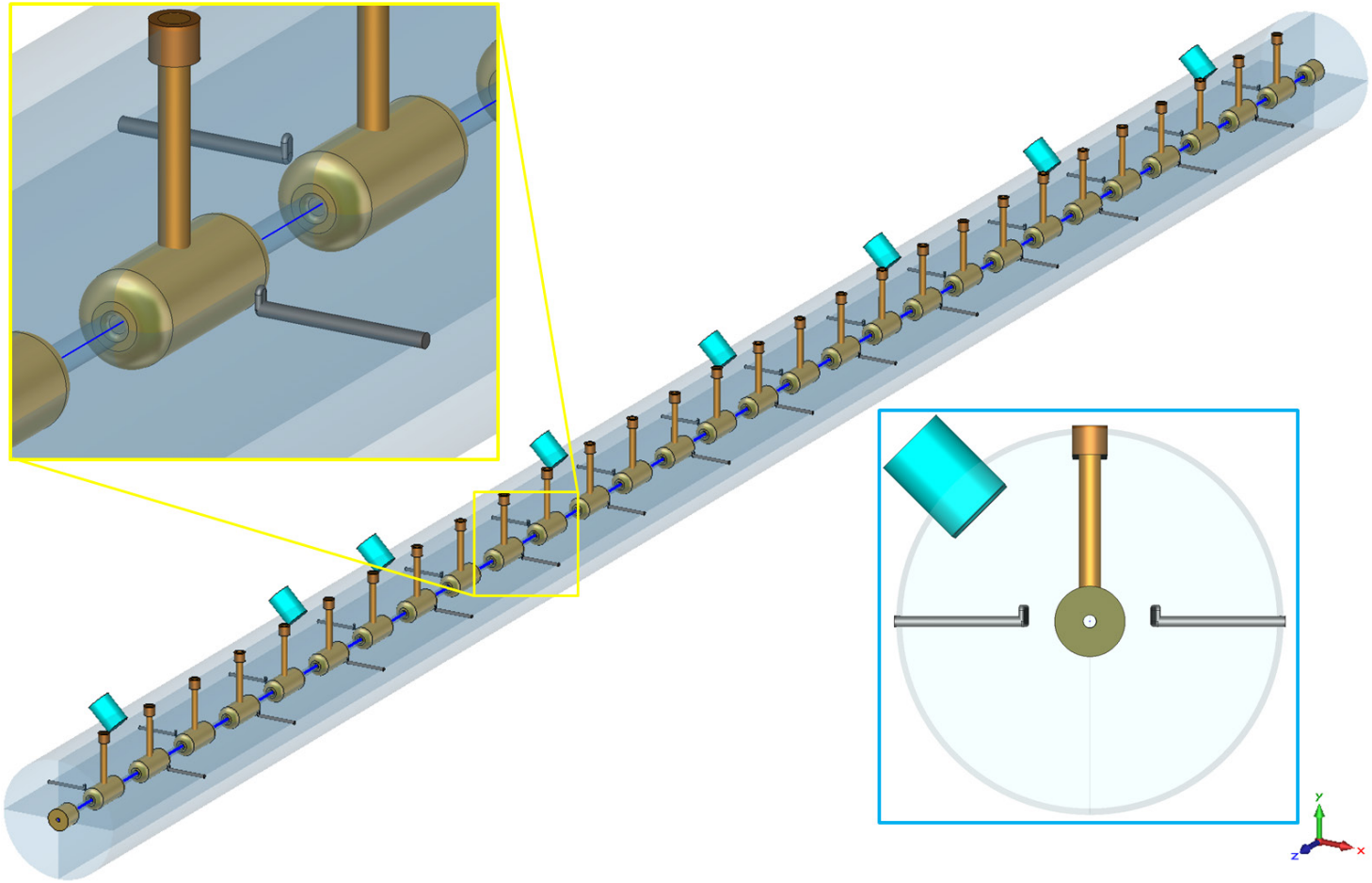

Frequency and field profile slug tuners in the DTL tank 4 model

# DTL exit beam

Results of PS simulations at the exit from the LANSCE DTL. One can notice the low-energy tail at ~20 MeV (~0.7% of initial particles) in additional to the regular bunches at 100 MeV (80.6% of initial). The tail beam velocity is ~½ of that in the bunches: m=2 acceleration.

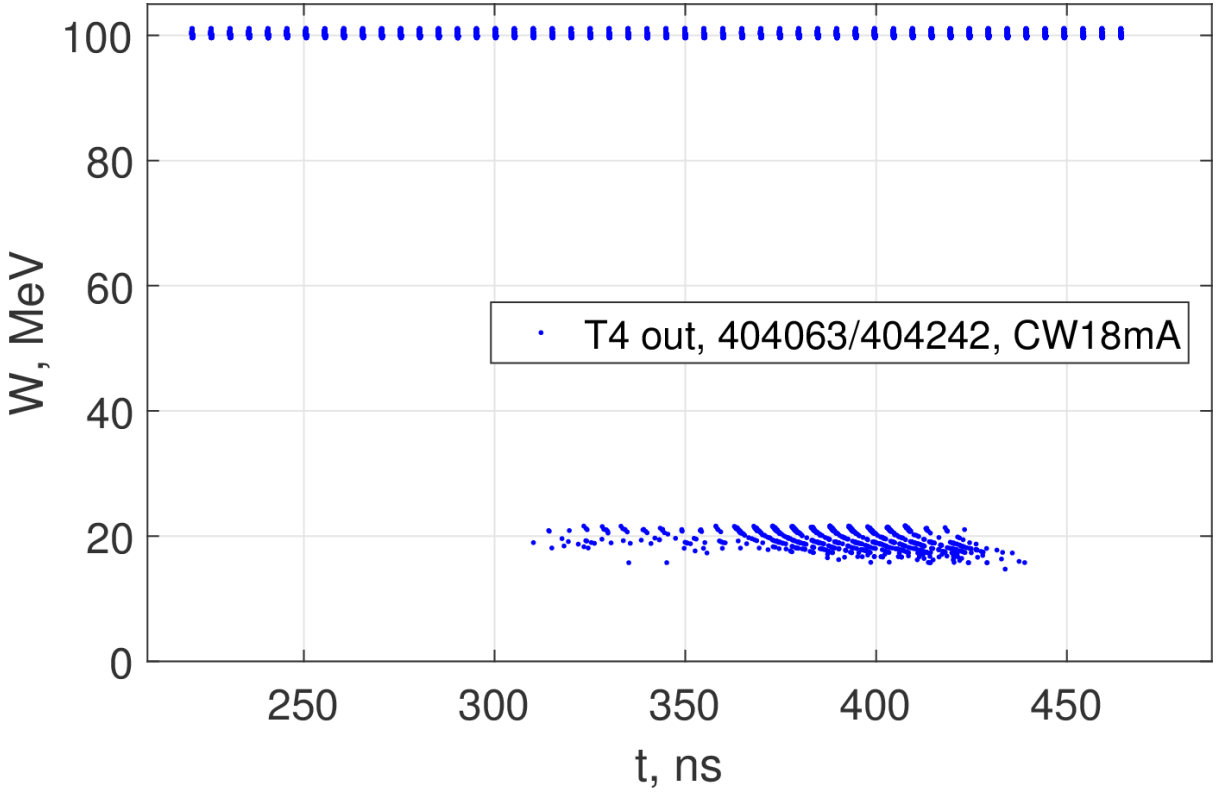


The particle energy at the exit of tank 4: 100 regular bunches and the m=2 tail from 10 RF periods.

# H-mode DTL

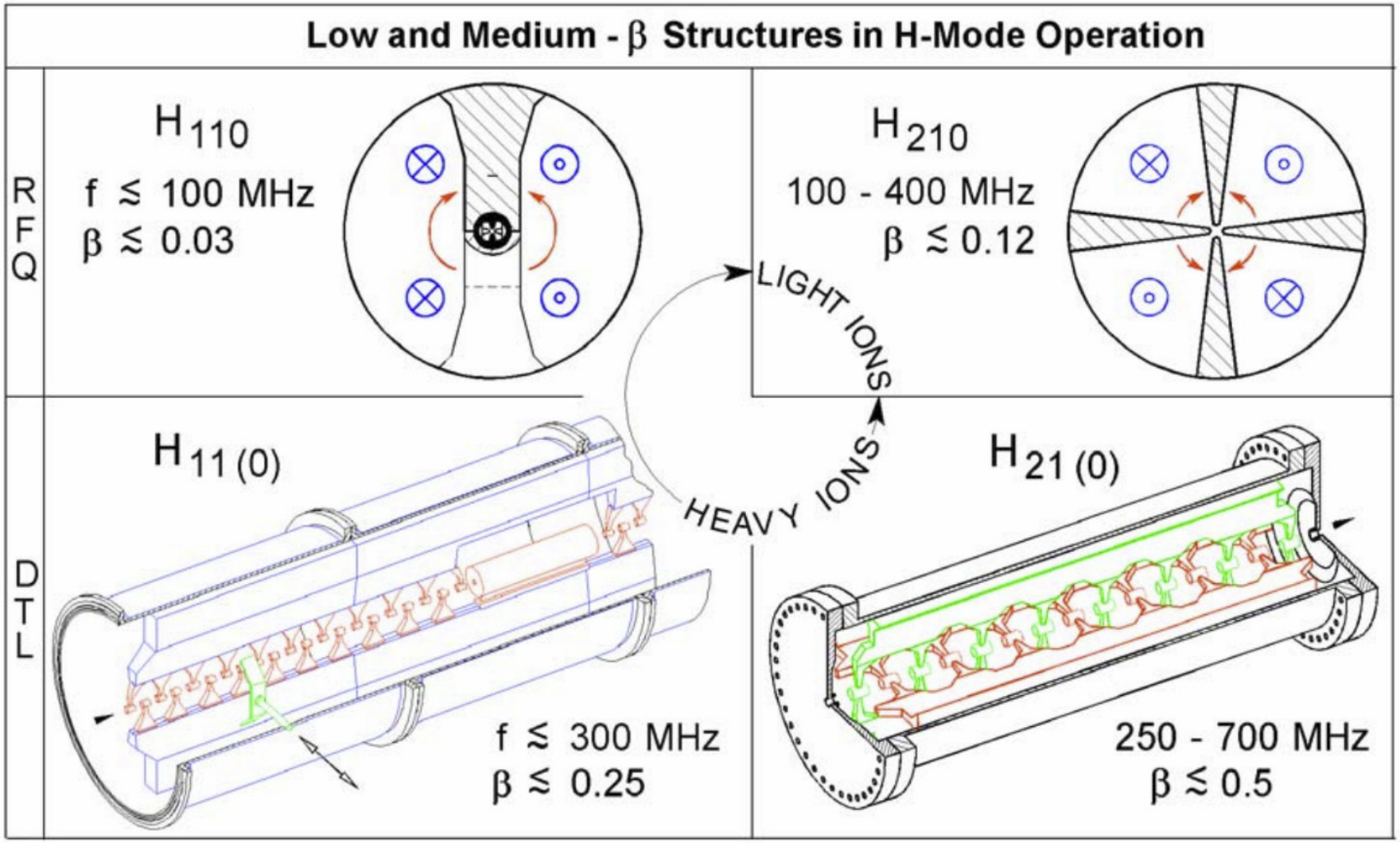


TE-mode DTL cavities: interdigital $H_{110}$ (IH) and cross-bar $H_{210}$ (CH)

# Coupled cells

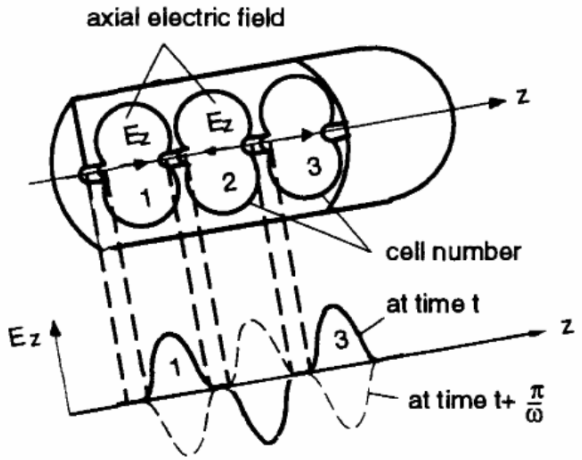


Standing wave accelerator operating in the $\pi$-mode

The structure can be considered as one resonator working in $\mu'=\pi p$ ($p$ = 0,1,2,..) mode.
In a resonator with $N$ cells $\mu'=\mu N$, where $\mu$ is the phase shift between cells. Then the phase shift between cells $\mu=\pi p/N$.

The mode frequencies are in the range

$$\frac{\omega_0}{\sqrt{1+k}} \le \omega \le \frac{\omega_0}{\sqrt{1-k}}$$

where $k<<1$ is the cell coupling coefficient.

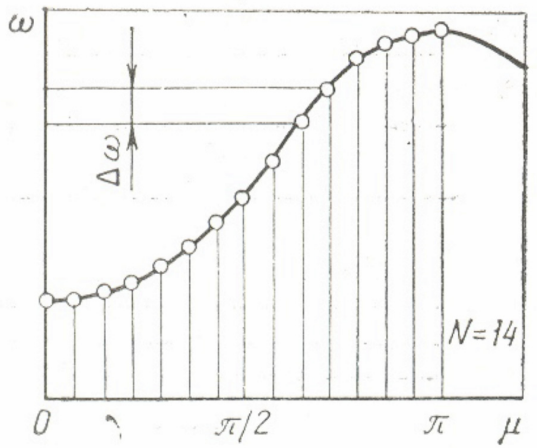


Dispersion curve of coupled cell structure: there are N+1 modes of oscillations in a structure containing N elements. The mode separation is maximal near $\pi/2$, so (a)→(c).

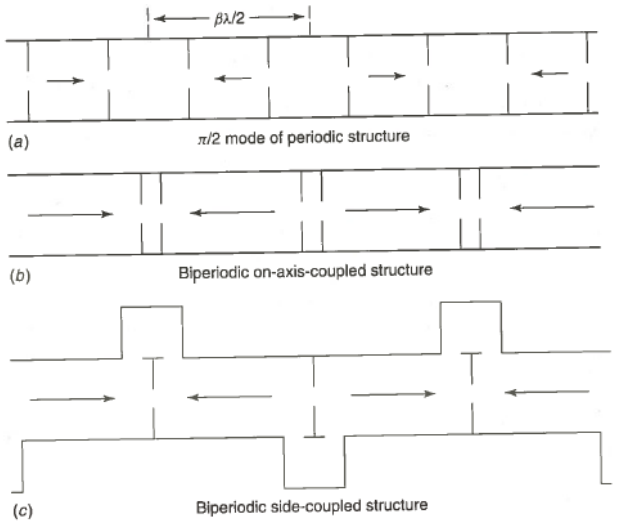

# Coupled-cell structures

Disk-loaded waveguide working in π-mode: weak coupling, sensitive to instability

Disk-loaded π-mode waveguide with additional magnetic coupling

Better coupling

Bi-periodic structures

Side-coupled structure

Disk and washer structure

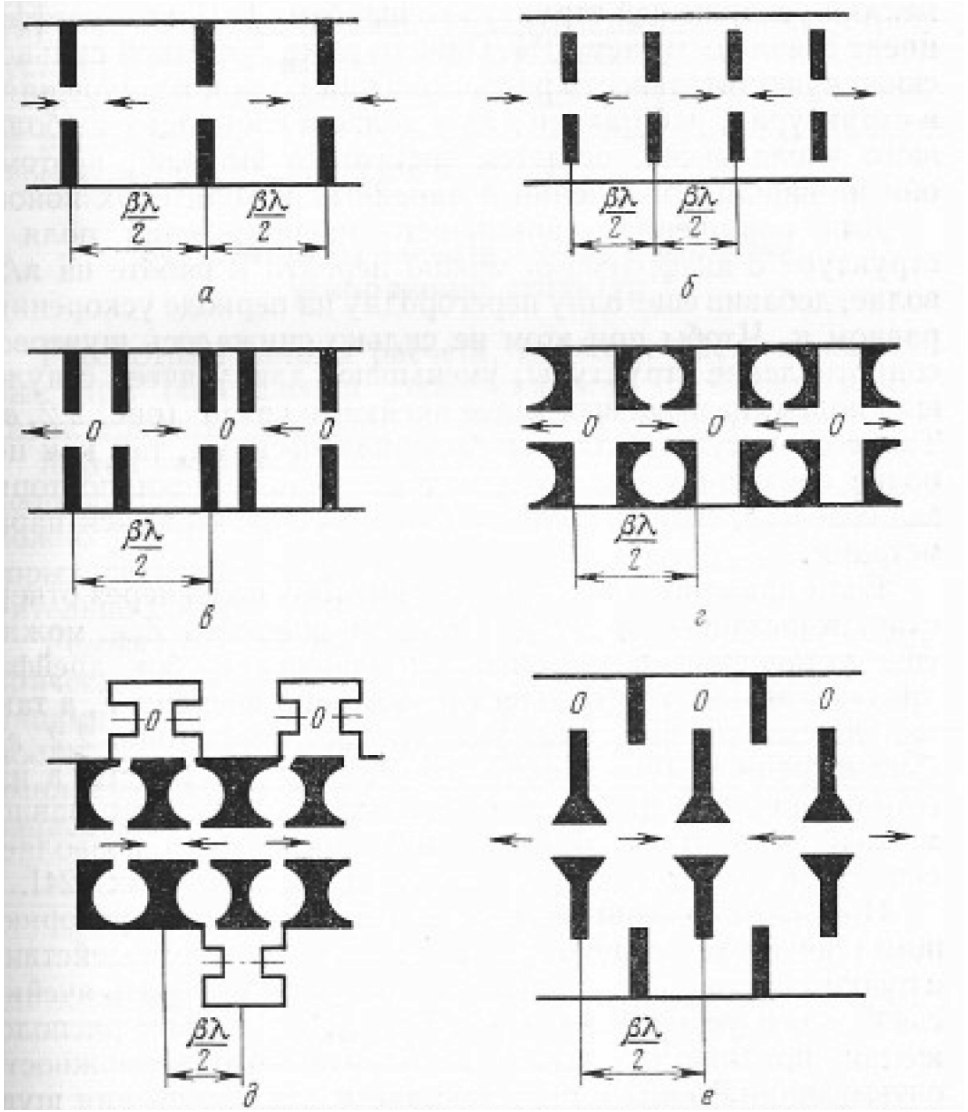

# Coupled-cavity linac (CCL)

The coupling cells are not excited when the structure is tuned.

Various types of CCL (see below) are used at relatively high velocities, typically for $\beta \geq 0.4$.

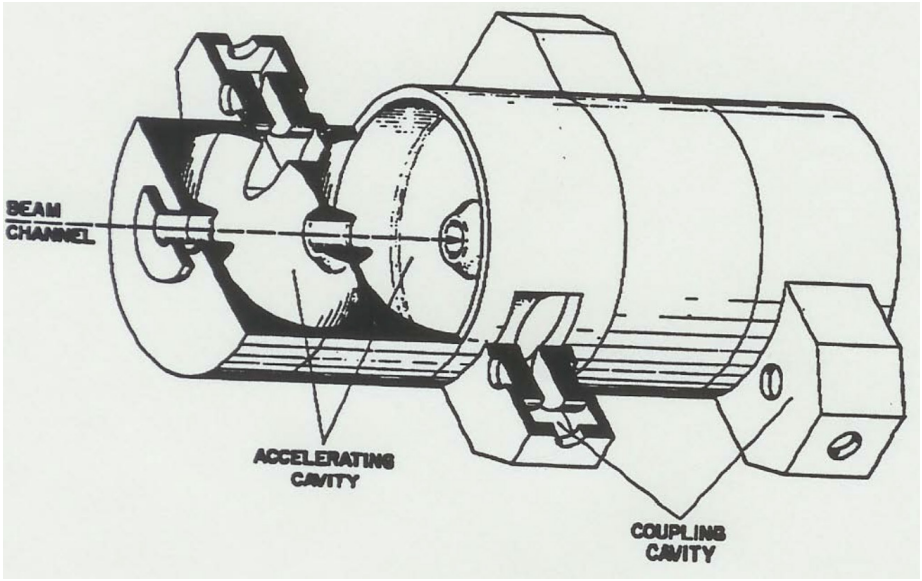


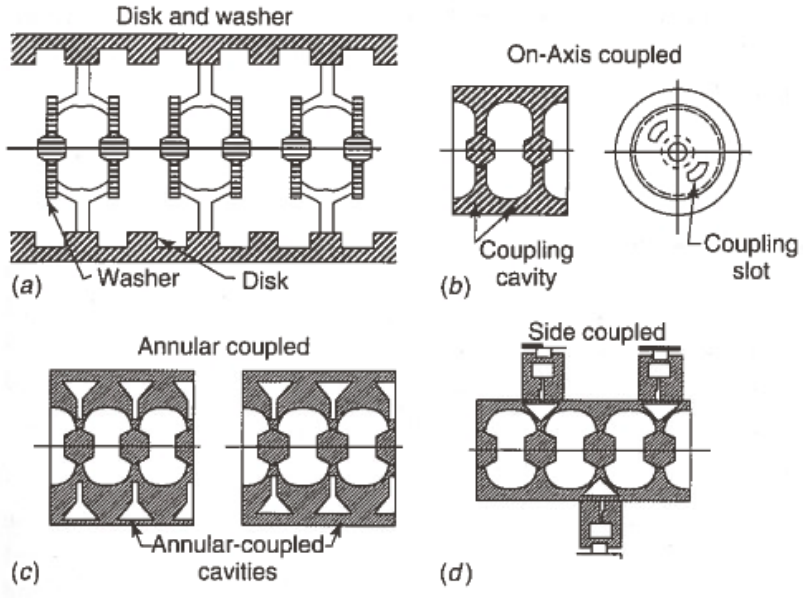


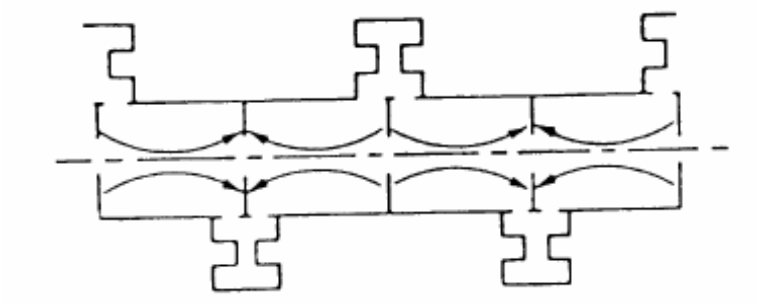

Energy range 100-800 MeV
High shunt impedance: 50 MΩ/m

Los Alamos Side Coupled Structure (1968)

# Shunt impedance of various accelerator structures vs β

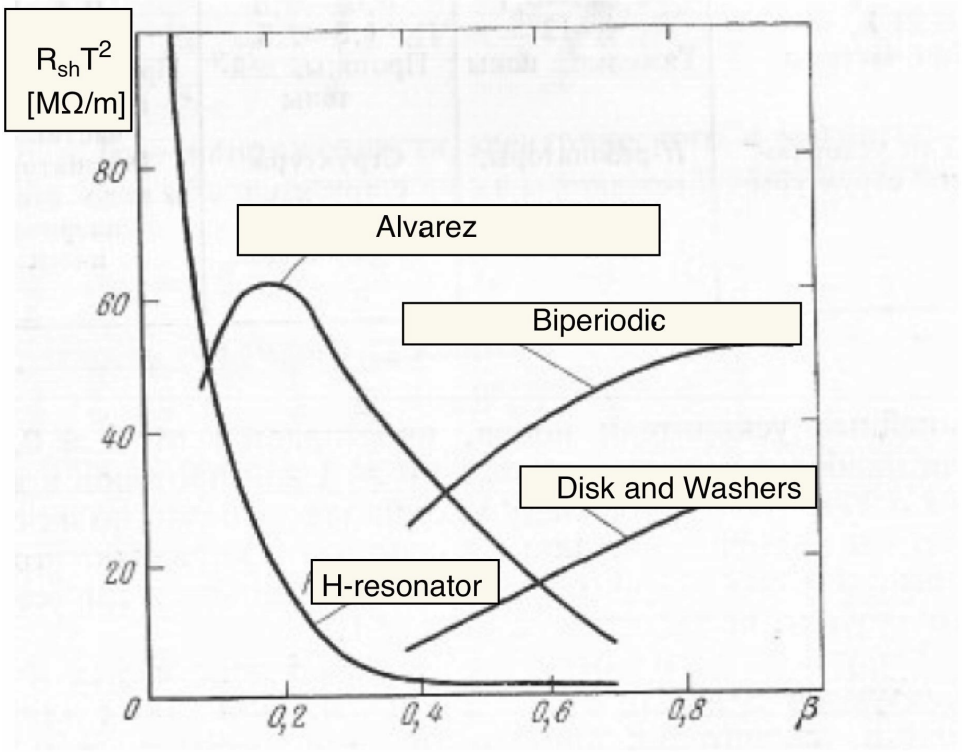


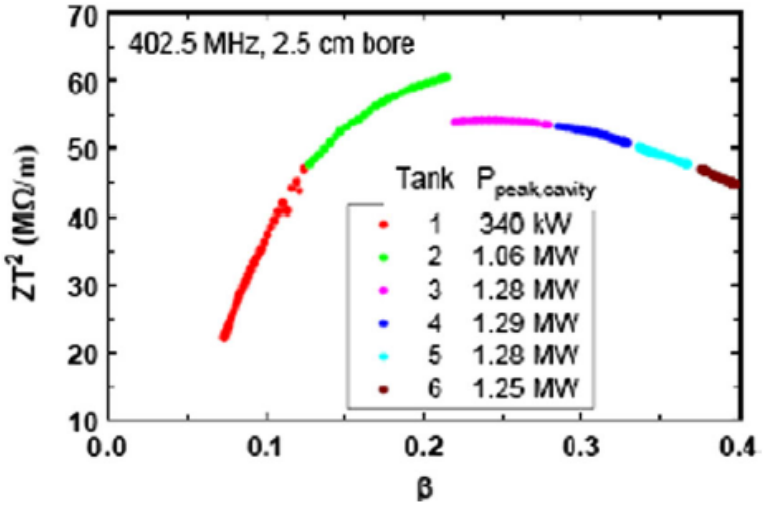


Effective shunt impedance of various normal-conducting structures versus *β* (left) and for 6 tanks of the SNS DTL (right).

# Independently Phased Cavities


Quarter-wave resonator

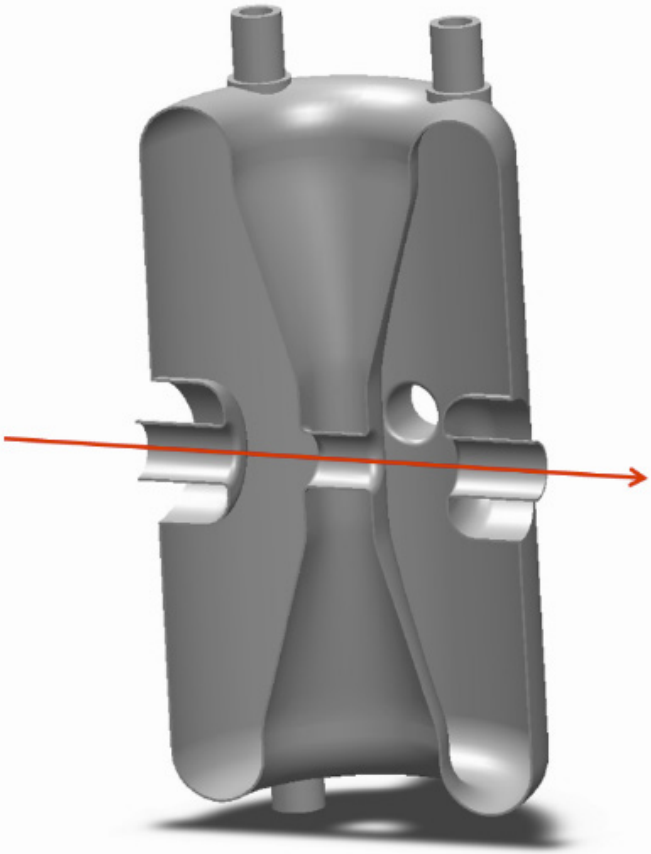

Half-wave resonator
a.k.a. spoke cavity

SC split-ring Nb
resonator (ANL)

Usually used at low frequencies and very low $\beta$, e.g. for heavy ions

# Spoke cavities (usually SC)

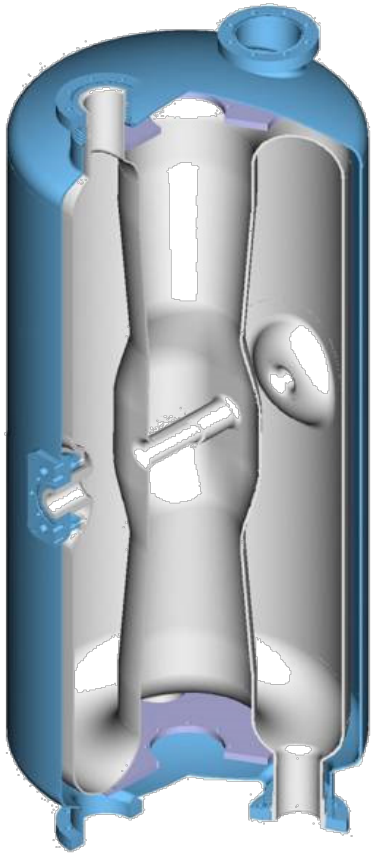

β=0.26

**Single spoke cavity =**
Half-wave resonator (HWR)

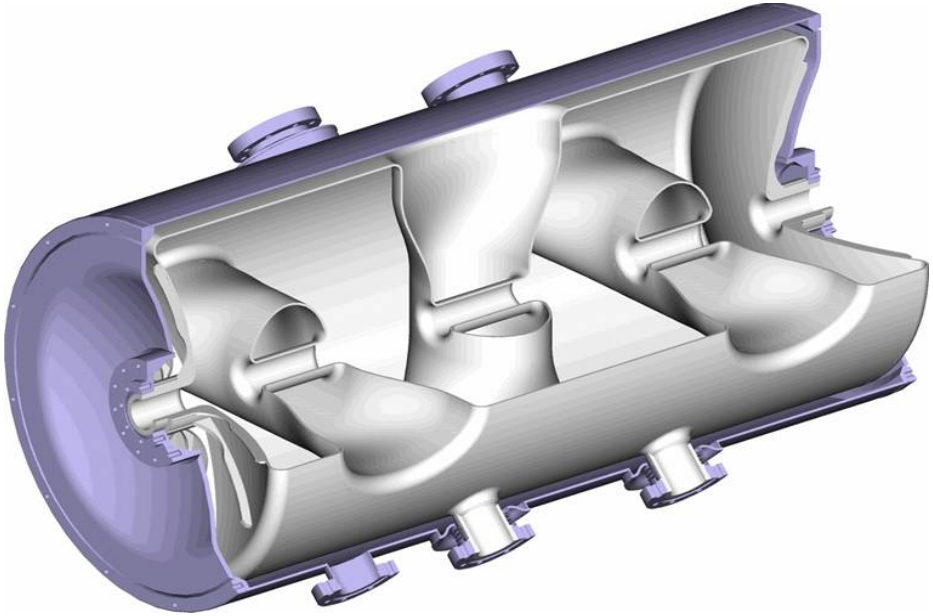

β=0.62

**Triple spoke cavity**

# Elliptical multi-cell SC cavities

High gradient:
10-20 MV/m
Compact design
Large aperture

Chain of cells electrically coupled ($ZT^2$ is not a concern)

Lower RF power requirement

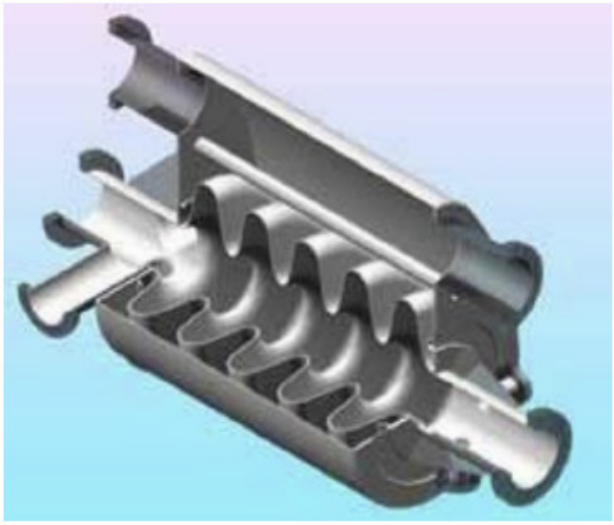

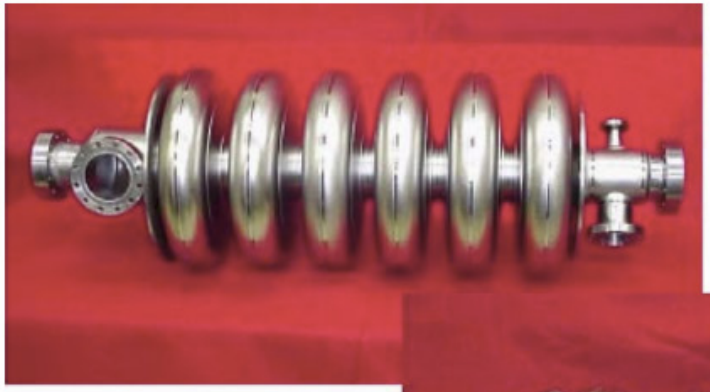

Six-cell 805-MHz medium-beta ($\beta$=0.61) and high-beta ($\beta$=0.81) SC niobium elliptical cavities. The SNS linac contains about 80 niobium cavities.

# Exotic things: accelerating muons

High-gradient linac of independent 0-mode cavities with external solenoid

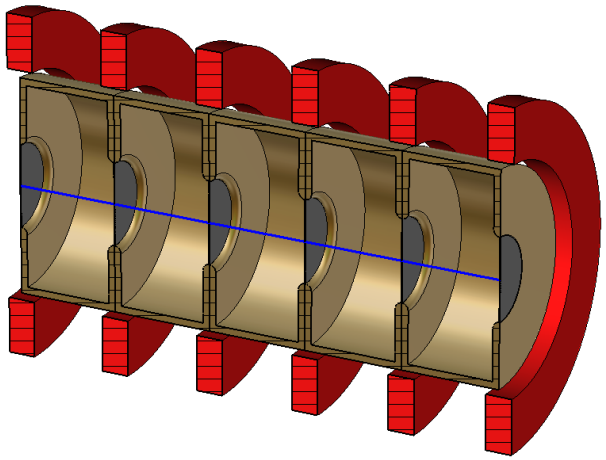

Muon-linac segment: 5 RF cavities (copper color) with thin-aperture windows (dark grey) surrounded by outer SC current coils (red).

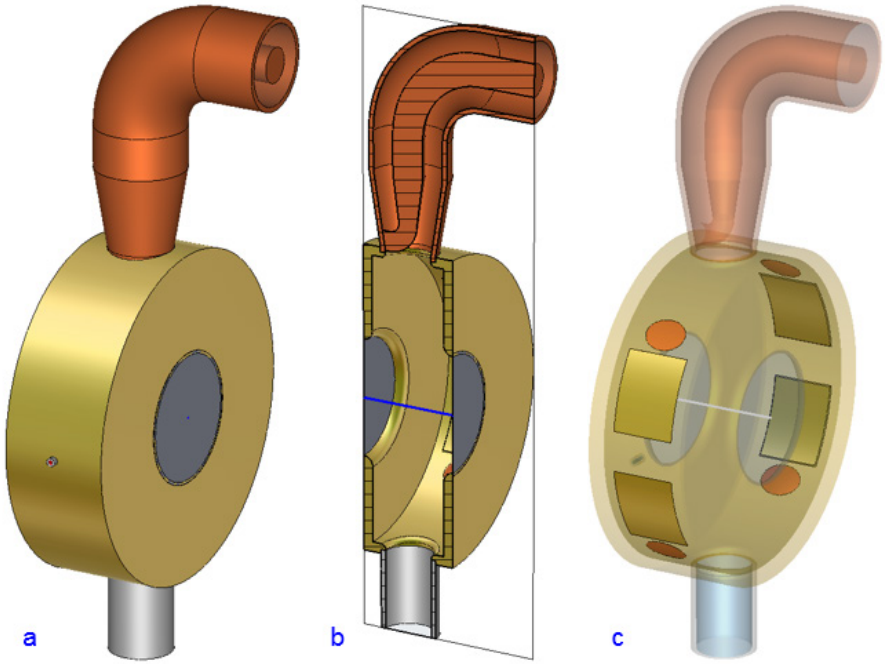


0-mode RF cavity for muons with thin-aperture windows (dark grey) and RF coupler. Tuning elements are highlighted in (c).

Muons penetrate the aperture windows. Such a linac with gradient 35 MV/m in solenoidal field of 5 T would accelerate muons to 200 MeV in 10 m.

# Exotic things: high-gradient accelerating structures

High-gradient (>100 MV/m) accelerating structures were developed for electrons (SLAC, CERN). They operate at high frequencies (X-band, 11-12 GHz) with very short RF pulses, 100s ns. Test cavity at 11.4 GHz, cut (below).

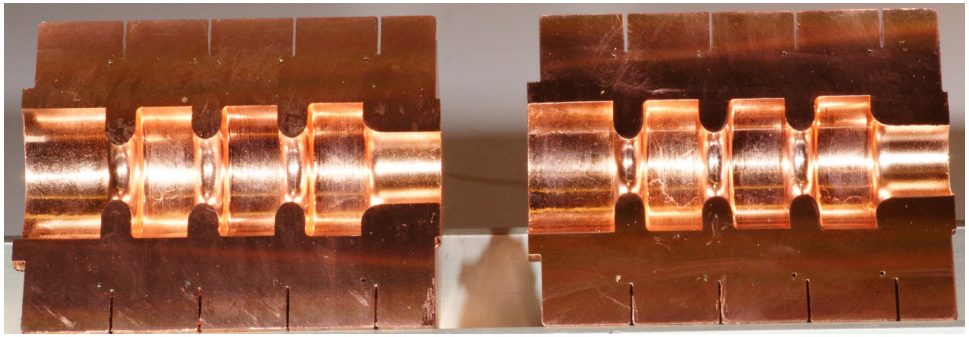

One can modify such cavities for protons: a HG proton booster after the existing linacs. Very low duty, short pulses, but it may work for some applications.

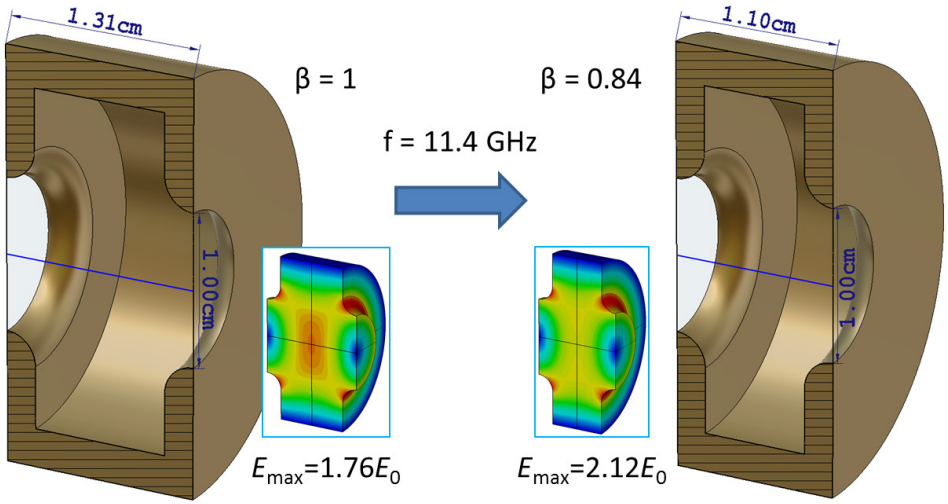

# Traveling wave (TW) accelerator structures

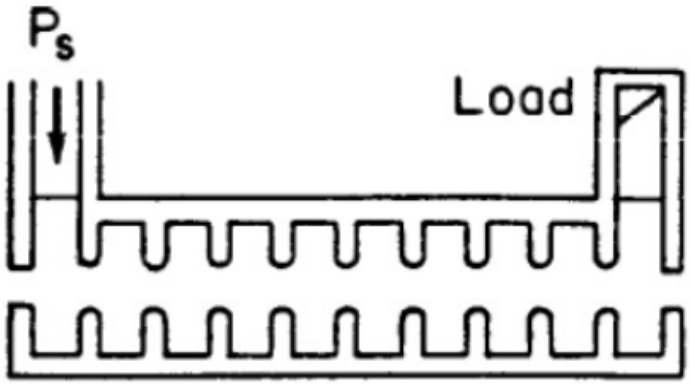


Linac with traveling wave. Primarily used for electrons.

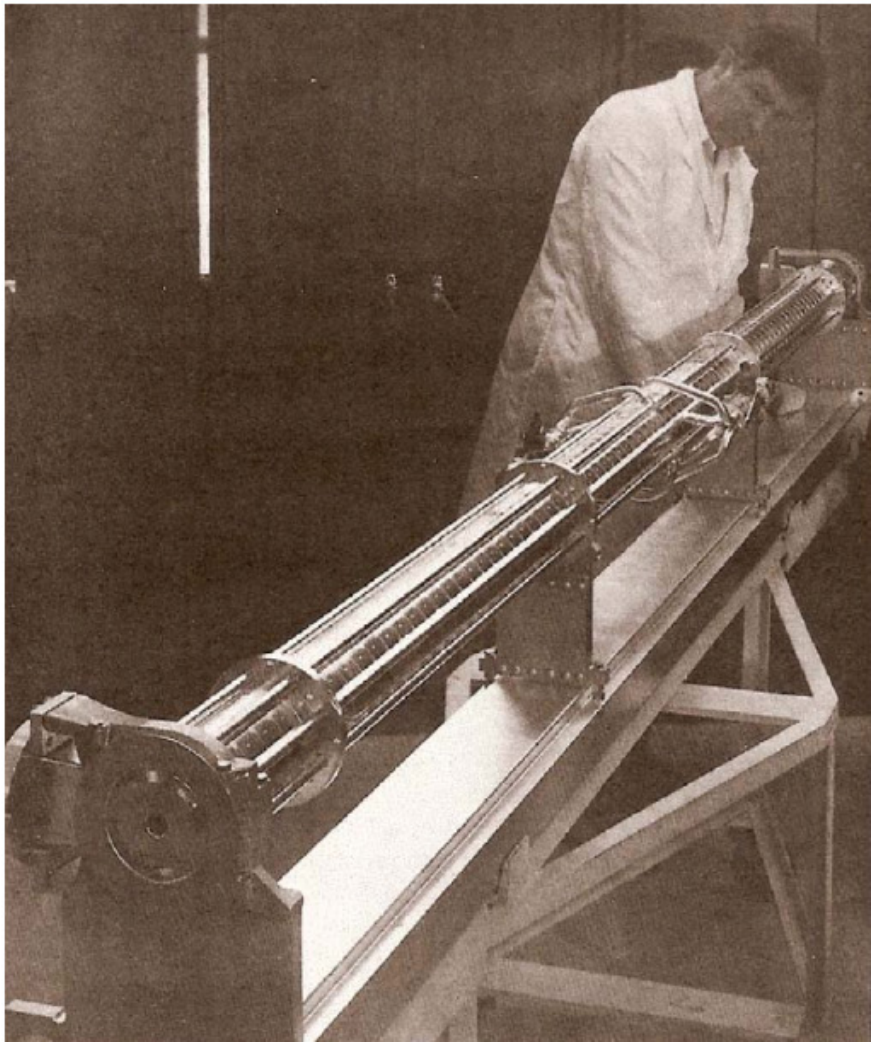

SLAC accelerating structure: 10-foot disk-loaded, 2856 MHz, 86 cells per structure, 960 structures make up the SLAC 3-km linac.

TW structures are usually used for electrons.

# TW accelerator structures vs SW

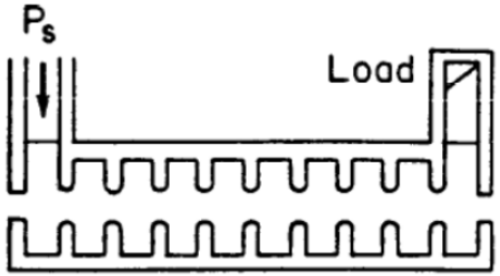


WG radius *b*
aperture radius *a*
aperture thickness *h*

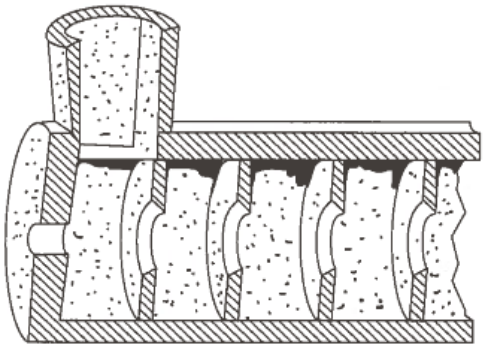

Constant-impedance TW structure: all cells are the same; $E_a(z) = E_0 e^{-\alpha_0 z}$.

Attenuation along the structure $\tau_0 = \alpha_0 L = \dfrac{\omega L}{2Qv_g}$, filling time $\tau_F = \dfrac{L}{v_g} = \tau_0 \dfrac{2Q}{\omega}$.

Energy gain $\Delta W = q\sqrt{2r_L P_0 L}\,\dfrac{1-e^{-\tau_0}}{\sqrt{\tau_0}}\cos\phi$, where $r_L = R_{sh}/L$. Optimum $\tau_0$=1.26.

Constant-gradient TW structure: cell parameters are adjusted to keep the same $E_a$.
SLAC linac: *b* is tapered from 4.2 cm to 4.1 cm, *a* from 1.3 cm to 1.0 cm; $\tau_0$=0.57.

Energy gain $\Delta W = q\sqrt{2r_L P_0 L\left(1-e^{-2\tau_0}\right)}\cos\phi$, filling time $\tau_F = \tau_0 \dfrac{2Q}{\omega}$.

TW structures are filled by energy “in space”: the EM field propagates along *z*.

In SW structures the EM field builds up “in time” everywhere in the structure.

# Summary of part 3

Linac accelerating structures are reviewed.
The structure choice depends on multiple factors: frequency, beam velocity range, required gradient, efficiency, operating duty factor, cost, etc.

Tools for designing structures:

- EM codes – Superfish (computer lab), or 3D codes (CST, HFSS, etc.)
- Beam dynamics codes – Trace, Parmila, Parmela, Beampath

Some codes are free and available for Los Alamos Accelerator Code Group at laacg.lanl.gov; others may be available at your universities or labs.